

Comprehensive analysis of sialylated N-glycans expressed in the
mouse cerebral cortex during development

Tomohiro Torii

Doctor of Philosophy

Department of Physiological Sciences, School of Life Sciences,
the Graduate University for advanced Studies
and
Division of Neurobiology and Bioinformatics,
National Institute for Physiological Sciences,
National Institutes of Natural Sciences

2007

Table and contents

Contents	2
Abstract	3
Abbreviations	5
Introduction	10
Materials and Methods	15
Results	26
Discussion	40
Conclusion	49
Acknowledgements	50
References	52
Legends to Figures	60
Figures	69
Tables	85

Abstract

Oligosaccharides of glycoprotein expressed on the cell surface play important roles in cell-cell interactions, particularly sialylated N-glycans with negative charge, which interact with sialic acid-binding lectins (siglecs). So far entire structure of sialylated N-glycans expressed in the mouse brain, particularly the linkage type of sialic acid residues to the backbone N-glycans, has not been elucidated. I improved the method to analyze pyridylaminated sugar chains using high performance liquid chromatography (HPLC) and determined the entire structure of sialylated N-linked sugar chains expressed in the mouse cerebral cortex during development. Three classes of sialylated sugar chains were mainly found. The most abundant class consisted of N-glycans containing α 2,3-sialyl linkages on a type 2 antennary (Gal β 1,4GlcNAc). Sialylated N-glycans with α 2,6-sialyl linkages on a type 2 antennary were present in the adult mouse cerebral cortex at a very low level as previously reported. However, I observed this structure to be abundantly expressed around birth, but only during this stage of development. This type of sialylated N-glycans forms receptor for human influenza virus, thus its temporal expression should add to our understanding of the

reason for higher incidence of influenza encephalitis among younger people. I also found a novel sialylated N-glycan with a [Gal β 1,3 (NeuAc α 2,6) GlcNAc -] structure, which was absent at embryonic day 12 but then increased during development. This new type of sialylated N-glycan structure comprised nearly 2% of the total N-glycans in the adult brain.

Additionally, I performed lectin histochemistry to confirm the results of HPLC analysis using α 2,3 or α 2,6 linkage sialic acid-recognizing lectin and determined the localization of these sialylated N-glycans in developing mouse cerebral cortices. N-glycans with α 2,3-sialyl linkage on a type 2 antennary detected by MMA lectin were ubiquitously expressed in the mouse brain during development. On the other hand N-glycans with α 2,6-sialyl linkage on a type 2 antennary temporary were expressed in microglia in addition to blood vessel.

Thus, the linkage and expression levels of sialylated N-glycans change dramatically during development.

Abbreviations

The nomenclature of oligosaccharide structures is as follows: An (where n = 0-2) indicates the number of antennae linked to the trimannosyl core (M3B); Gn (where n = 0-4), the number of galactose residues attached via β 1,4 linkage to non-reducing ends; G'n (where n = 1-2), the number of galactose residues attached via β 1,3 linkage to the non-reducing ends; F, with core fucosylation; Fo, with outer arm fucosylation attached via β 1,3 linkage to *N*-acetylglucosamine residues; B, with bisecting *N*-acetylglucosamine residues.

Isobaric monosaccharide composition: H=hexose (Galactose, mannose),
N=N-acetylhexosamine, F=Fucose

Abbreviations and structures of PA-sugar chains (continue).

Abbreviation	structure
H5.1	$\begin{array}{c} \text{Man } \alpha 1 \backslash \\ \text{Man } \alpha 1 \backslash \quad \text{Man } \alpha 1 \backslash \\ \text{Man } \alpha 1 \backslash \quad \text{GlcNAc } \beta 1-4 \text{ Man } \beta 1-4 \text{ GlcNAc } \beta 1-4 \text{ GlcNAc-PA} \\ \text{GlcNAc } \beta 1-2 \text{ Man } \alpha 1 \end{array}$
A0G0	$\begin{array}{c} \text{Man } \alpha 1 \backslash \\ \text{Man } \alpha 1 \backslash \quad \text{Man } \beta 1-4 \text{ GlcNAc } \beta 1-4 \text{ GlcNAc-PA} \\ \text{Man } \alpha 1 \end{array}$
A0G0F	$\begin{array}{c} \text{Man } \alpha 1 \backslash \\ \text{Man } \alpha 1 \backslash \quad \text{Man } \beta 1-4 \text{ GlcNAc } \beta 1-4 \text{ GlcNAc-PA} \\ \text{Man } \alpha 1 \quad \text{Fuc } \alpha 1 \\ \quad \quad \quad \\ \quad \quad \quad 6 \end{array}$
A1(6)G0F	$\begin{array}{c} \text{GlcNAc } \beta 1-2 \text{ Man } \alpha 1 \backslash \\ \text{Man } \alpha 1 \backslash \quad \text{Man } \beta 1-4 \text{ GlcNAc } \beta 1-4 \text{ GlcNAc-PA} \\ \text{Man } \alpha 1 \quad \text{Fuc } \alpha 1 \\ \quad \quad \quad \\ \quad \quad \quad 6 \end{array}$
BA-1	$\begin{array}{c} \text{GlcNAc } \beta 1-2 \text{ Man } \alpha 1 \backslash \\ \text{GlcNAc } \beta 1-4 \text{ Man } \beta 1-4 \text{ GlcNAc } \beta 1-4 \text{ GlcNAc-PA} \\ \text{Man } \alpha 1 \quad \text{Fuc } \alpha 1 \\ \quad \quad \quad \\ \quad \quad \quad 6 \end{array}$
A2G0B	$\begin{array}{c} \text{GlcNAc } \beta 1-2 \text{ Man } \alpha 1 \backslash \\ \text{GlcNAc } \beta 1-4 \text{ Man } \beta 1-4 \text{ GlcNAc } \beta 1-4 \text{ GlcNAc-PA} \\ \text{GlcNAc } \beta 1-2 \text{ Man } \alpha 1 \end{array}$
BA-2	$\begin{array}{c} \text{GlcNAc } \beta 1-2 \text{ Man } \alpha 1 \backslash \\ \text{GlcNAc } \beta 1-4 \text{ Man } \beta 1-4 \text{ GlcNAc } \beta 1-4 \text{ GlcNAc-PA} \\ \text{GlcNAc } \beta 1-2 \text{ Man } \alpha 1 \quad \text{Fuc } \alpha 1 \\ \quad \quad \quad \quad \quad \\ \quad \quad \quad \quad \quad 6 \end{array}$
A2G'2F	$\begin{array}{c} \text{Gal } \beta 1-3 \text{ GlcNAc } \beta 1-2 \text{ Man } \alpha 1 \backslash \\ \text{Gal } \beta 1-3 \text{ GlcNAc } \beta 1-2 \text{ Man } \alpha 1 \backslash \quad \text{Man } \beta 1-4 \text{ GlcNAc } \beta 1-4 \text{ GlcNAc-PA} \\ \text{Gal } \beta 1-3 \text{ GlcNAc } \beta 1-2 \text{ Man } \alpha 1 \quad \text{Fuc } \alpha 1 \\ \quad \quad \quad \quad \quad \\ \quad \quad \quad \quad \quad 6 \end{array}$
A1G1FoFB	$\begin{array}{c} \text{Gal } \beta 1-4 \text{ GlcNAc } \beta 1-2 \text{ Man } \alpha 1 \backslash \\ \text{Fuc } \alpha 1 \backslash \quad \text{Man } \beta 1-4 \text{ GlcNAc } \beta 1-4 \text{ GlcNAc-PA} \\ \text{GlcNAc } \beta 1-2 \text{ Man } \alpha 1 \quad \text{Fuc } \alpha 1 \\ \quad \quad \quad \quad \quad \\ \quad \quad \quad \quad \quad 6 \end{array}$
A2G2	$\begin{array}{c} \text{Gal } \beta 1-4 \text{ GlcNAc } \beta 1-2 \text{ Man } \alpha 1 \backslash \\ \text{Gal } \beta 1-4 \text{ GlcNAc } \beta 1-2 \text{ Man } \alpha 1 \backslash \quad \text{Man } \beta 1-4 \text{ GlcNAc } \beta 1-4 \text{ GlcNAc-PA} \\ \text{Gal } \beta 1-4 \text{ GlcNAc } \beta 1-2 \text{ Man } \alpha 1 \end{array}$
A2G2F	$\begin{array}{c} \text{Gal } \beta 1-4 \text{ GlcNAc } \beta 1-2 \text{ Man } \alpha 1 \backslash \\ \text{Gal } \beta 1-4 \text{ GlcNAc } \beta 1-2 \text{ Man } \alpha 1 \backslash \quad \text{Man } \beta 1-4 \text{ GlcNAc } \beta 1-4 \text{ GlcNAc-PA} \\ \text{Gal } \beta 1-4 \text{ GlcNAc } \beta 1-2 \text{ Man } \alpha 1 \quad \text{Fuc } \alpha 1 \\ \quad \quad \quad \quad \quad \\ \quad \quad \quad \quad \quad 6 \end{array}$

GlcNAc:	N-acetylglucosamine
Man:	mannose
Gal:	galactose
Fuc:	fucose
E12:	embryo day 12
12w:	12 weeks
GU:	glucose unit
MU:	mannose unit
CNS:	central nervous system
HPLC:	high performance liquid chromatography
MALDI/TOF-MS:	matrix-assisted laser-desorption ionization time-of-flight massspectrometer
RA:	relative abundance
SVZ:	subventricular zone
PA-:	pyridylamino
ODS:	octadecyl silica.

Introduction

Sugar chains envelop a vast majority of the cell surface and are considered to play significant roles in cell-cell and extracellular matrix interactions as mediators and signal transducers. Increasing evidence suggested that glycosylation have crucial roles in various biological functions and require coordinated action of glycosyltransferases (Lau *et al.* 2006; Ohtsubo *et al.* 2006). Others and we have studied developmental changes in the gene expression of sugar chain-metabolizing enzymes and the structure of glycoconjugates, and found that the expression of glycoconjugates including N-glycans and glycosphingolipids changes dramatically during development (Ishii *et al.* 2007; Ngamukote *et al.* 2007), differentiation (Hakomori 1981), and oncogenic transformation (Miyoshi *et al.* 1993). Sialic acids and their derivatives are ubiquitous at the terminal positions of oligosaccharides of glycoproteins and glycolipids in tissues of various animal species. So far, however, we have been analyzing the structure of N-linked sugar chains after removal of sialic acid residues because of complexity of analysis.

In the rodent brain, 40% of total N-glycan is sialylated and approximately

10% of the N-glycan carries polysialic acids, a part of which contains PSA on N-CAM (Zamze *et al.* 1998). Growing evidence suggests that the structure containing sialic acid plays particularly important roles in cell-cell or extracellular matrix interaction. Proteins that recognize and bind to a certain structure of sugar chains are called lectins, but within the lectin, those that bind to sialic acid-containing structure is particularly named “siglec (sialic acid-binding immunoglobulin-like lectin family)” demonstrating the significance of this type of lectin. Siglecs can recognize not only the sialic acid residue but also the sugar residue next to it (Crocker *et al.* 2002; Fischer and Brossmer 1995). They also distinguish the linkage between sialic acid and the next sugar residue (Attril *et al.* 2006). Thus, siglecs that bind to α 2,3-sialic acid are distinct from those bind to α 2,6-sialic acid. The α 2,3-sialic acid binding proteins, such as CHL1, NrCAM, and NgCAM, belong to the L1 super-family and they have all been shown to be neurite outgrowth promoters and/or mediators of neuron–glia interactions (Kleene and Schachner 2004). Myelin-associated glycoprotein (MAG), a member of siglecs, is involved not only in myelin formation, but also in myelin maintenance (Schachner and Bartsch 2000). It has received particular attention because it enhances in vitro neurite

outgrowth at early developmental stages, but inhibits neurite outgrowth in the adult (Vyas *et al.* 2005), thereby possibly contributing to the non-conducive environment for regeneration in the adult mammalian CNS. Therefore, it is extremely important to determine the structure of sialic acid-containing sugar chain in the adult brain as well as those during development to understand the significance of interaction among siglecs and sialic acid-containing sugar chains. The structure of gangliosides is well analyzed and their developmental profile of expression is known, however, that of N-linked sugar chains is poorly understood.

In one report, structure of sialylated N-linked sugar chains in the adult rat brain has been thoroughly analyzed and quantified (Zamze *et al.* 1998). They reported that sialylated N-glycans predominantly carry α 2,3-linked sialic acid, with little or no α 2,6-linked sialic acid in the adult brain. Also they have determined the structure of most of the sialic acid-containing N-linked sugar chains. However, their quantification of each sugar chain was done by MALDI-TOF mass spectrometry, by which comparison of the quantity of different substances is difficult since ionization efficiency differs among the different substances, and they have not studied developmental profile

of sugar chains. Moreover, there is a critical lack of information in the structure of N-linked sugar chains they presented: the linkage of sialic acid bound to each sugar chain was not determined because they performed permethylation analysis of entire brain sugar chains without purification for the linkage analysis.

We have been developing a systematic method to analyze the N-linked sugar chain expression pattern present in a whole tissue without glycoprotein purification after removal of sialic acid residues (Hase *et al.* 1981; 1987; 1994; 1998; Fujimoto *et al.* 1999; Tanabe and Ikenaka 2006). Ishii *et al.* (2007) revealed that (i) the expression pattern of the N-linked sugar chains changes dramatically during developmental stages of the mouse cerebral cortex, (ii) the expression pattern of N-linked sugar chains are well conserved among individuals. Ishii *et al.* (2007) also established cDNA macroarray system capable of evaluating the expression of many glycosidase and glycosyltransferase genes (116 genes) derived from developmental mouse cerebral cortex and the other tissues. Based on these results, they suggested that the expression patterns of N-linked sugar chains are strictly regulated in a spatiotemporal manner. However, they have not analyzed structure and expression level of sialylated N-glycans.

Here, I established a method to analyze sialic acid-containing N-linked sugar chains, and systematically analyzed expression level and linkage of sialylated N-glycans in the developing mouse cerebral cortex using this system. I have identified a new sialic acid-containing structure in the brain and demonstrated that α 2,6-sialic acid-containing structure is abundantly expressed during development. These results demonstrate that the interaction among siglecs and sialic acid-containing sugar chains is dynamically changing during development.

Materials and methods

Materials

Various standard PA-sugar chains for 2D-mapping analysis were purchased from Takara (Japan) or Seikagaku Corporation (Japan).

A scheme presenting entire protocol for extracting and purification of pyridylaminated sugar chain is shown in Fig. 1.

Pyridylation of sugar chains released from tissue samples

ICR mice of various developmental stages (E12, E16, P0, P7) or adult (12w) were sacrificed, and their cerebral cortices were quickly removed and washed with ice-cold PBS (-). Tissues were homogenized in a nine-fold volume of acetone using a Polytron homogenizer. After being placed on ice at least for 1 hour, the homogenate was centrifuged at 2,150g for 20 min and the pellet was dried in a spinvac centrifuge.

A lyophilized sample (2 mg) was hydrazinolized (100°C, 10 h) followed by N-acetylation as previously reported (Tanabe and Ikenaka 2006).

Graphite carbon column

Hydrazine solution was mixed with 3 ml of 50 mM ammonium acetate buffer (pH 7.0) and loaded onto a graphite carbon column. After the column was washed with 15 ml of a 50 mM ammonium acetate buffer (pH 7.0), oligosaccharides were eluted with 5 ml of a mixed solution A [50 mM triethylamine acetate buffer (pH 7.0)/acetonitrile containing 2% acetic anhydride (40:60, v/v)]. All of these processes were carried out using a vacuum chamber (GL Science). After samples were dried, N-acetylated oligosaccharides were obtained in a glass tube.

Pyridylation

Purified glycans were tagged with a fluorophore, 2-aminopyridine, as described (Hase *et al.* 1981; 1987; 1994; 1998; Fujimoto *et al.* 1999; Tanabe and Ikenaka 2006). After graphite carbon column treatment, dried oligosaccharides derived from glycoprotein were heated with 20 μ l of a pyridylation reagent (prepared by mixing 138 mg 2-aminopyridine and 50 μ l acetic acid) at 90°C for 60 min. The Schiff base was reduced by heating with 70 μ l of a reducing reagent (freshly prepared by mixing 200

mg dimethylamine-borane complex, 50 μ l water, and 80 μ l acetic acid) at 80°C for 35 min. The pyridylaminated sugar chains were loaded onto a cellulose column for removing excess reagents.

Cellulose column

Excess reagents were removed by using a cellulose cartridge column (Takara, Japan) according to the manufacture's instructions with minor modifications. The pyridylaminated sugar chains were mixed with 3 ml of solution 1 [1-butanol/ethanol/0.6 M acetic anhydride (4:1:1, v/v)] and loaded onto a cellulose column. After the column was washed with 15 ml of a solution 1, oligosaccharides were eluted with 5 ml of a mixed solution 2 [75 mM sodium bicarbonate solution/ethanol (2:1, v/v)]. All of these processes were carried out using a vacuum chamber (GL Science). The eluted solution was dried and PA-oligosaccharides were obtained in a glass tube.

Sugar chain analysis and separation by HPLC

Analyses of PA-sugar chains using HPLC were performed essentially as reported

previously with some modifications. Briefly, sialylated PA-sugar chains were separated on MonoQ ER5/5 column (5×50 mm; Amersham Biosciences, USA), which was performed as the initial step to separate sialylated oligosaccharides according to their negative charges. MonoQ HPLC was performed on a MonoQ ER5/5 column at a flow rate of 1.0 ml/min at room temperature. Solvent A consisted of distilled H₂O titrated to pH 9.0 with 1 M aqueous ammonia, and solvent B consisted of 0.5 M ammonium acetate (pH 9.0). After injecting a sample, proportion of solvent B was increased linearly to 12% in 3 min, to 40% in 14 min, and then to 100% in 5 min. PA-sugar chains were detected at an excitation wavelength of 310 nm and emission wavelength of 380 nm.

Total and fractionated sialylated N-glycans, which were digested with *Arthrobacter ureafaciens* sialidase (Nacalai Tesque, Japan) were analyzed and size fractionated from M2 to M11 according to the mannose unit standards (TaKaRa, Japan) on an Asahipak NH2P-50 column (Shodex, Japan). PA-sugar chains were detected by a fluorescence detector (FP-2025; Jasco, Japan). Each HPLC step was performed as described below.

Size-fractionation HPLC was performed on an Asahipak NH2P-50 column at a flow rate of 0.6 ml/min at 30°C. Solvent C consisted of 93% acetonitrile, 0.3% acetic acid titrated to pH 7.0 with 1 M aqueous ammonia, and solvent D consisted of 20% acetonitrile, 0.3% acetic acid titrated to pH 7.0 with 1 M aqueous ammonia. The column was equilibrated with mixtures of solvent C and solvent D (ratio 80:20), increased linearly to 58% in 180 min and then to 80% in 5 min. PA-sugar chains were detected at an excitation wavelength of 310 nm and an emission wavelength of 380 nm.

Reverse-phase HPLC was performed on a Develosil C30-UG-5 column (Nomura Chemical, Japan) at a flow rate of 0.5 ml/min at 30°C. Solvent E consisted of 3.77 mM ammonium acetate buffer (pH 4.0), and solvent F was composed of solvent E containing 10 % acetonitrile. The column was equilibrated with mixtures of solvent E and solvent F (ratio 80:20), its ratio increased linearly to 42% in 60 min, and then to 80% in 5 min. PA-sugar chains were detected at an excitation wavelength of 320 nm and an emission wavelength of 400 nm.

Reverse-phase HPLC for purification of sialylated N-glycans was performed on a Develosil ODS-5 column (4.6×250 mm) at a flow rate of 1.0 ml/min. The

column was equilibrated with 20 mM ammonium acetate buffer titrated to pH 4.0 with triethylamine containing 0.05% 1-butanol. After injecting a sample, the concentration of 1-butanol was increased linearly to 0.4% over 90 min. PA-sugar chains were detected at an excitation wavelength of 320 nm and an emission wavelength of 400 nm.

Quantification of PA-sugar chains

Digital chart recorder, Power ChromTM (AD Instruments, NSW, Australia) or MacIntegratorTM (Rainin Instruments, MA, USA) system running on MacintoshTM computers (Apple Computer, CA, USA) and UnipointTM (Gilson Inc. USA) System Software Version 3.1 running on Microsoft Windows® were used for analysis of area and elution times of each peak. The amount of N-linked sugar chains contained in each tissue was quantified by adding the peak areas from all the fractions (M3-M11). The amount of each sugar chain was expressed as the molar percentage of total N-linked sugar chains.

Matrix-assisted laser-desorption ionization time-of-flight mass spectrometry

(MALDI/TOF-MS)

The molecular mass of PA-sugar chains and their isobaric monosaccharide composition were determined by MALDI/TOF-MS.

The PA-sugar chains were dissolved in water. One ml of matrix solution (10 mg/ml 2,5-dihydroxybenzoic acid in 30% acetonitrile) were deposited onto a stainless steel target and analyzed after being dried rapidly. MALDI/TOF mass spectra of the samples were acquired using a REFREXTM spectrometer (Bruker-Franzen, Germany) in the positive and reflector mode at an acceleration voltage of 20 kV and delayed ion extraction. Standard PA-sugar chains were used to achieve a two-point external calibration for mass assignment of ions. The mass spectra shown are the sum of at least 30 laser shots.

Exoglycosidase digestion

Purified PA-N-glycan were digested in a volume of 20 ml for 12 h at 37°C using each enzyme. *Diplococcus pneumoniae* β -galactosidase (Roche Diagnostics, Basel, Switzerland), specific for β (1,4)Gal, 50 mU/ml in 50 mM sodium acetate pH 6.0; jack

bean β -galactosidase (Seikagaku Corporation, Tokyo, Japan), specific for $\beta(1,3/4)\text{Gal}$, 5 mU/ml in 50 mM sodium citrate pH 3.5; $\alpha(1,3/4)\text{-L-fucosidase}$ (Takara, Japan), specific for $\alpha(1,3/4)\text{Fuc}$, 100 nU/ml in 50 mM sodium acetate pH 6.0; bovine kidney α -fucosidase (Glyco, Upper Heyford, UK), specific for $\alpha(1,6>1,2/3/4)\text{Fuc}$, 1 mU/ml in 100 mM sodium citrate/phosphate pH 6.0; jack bean α -mannosidase (Seikagaku Corporation, Tokyo, Japan), specific for $\alpha(1,2/3/6)\text{Man}$, 12.5 mU/ml in 100 mM sodium acetate pH 4.5 containing 1 mM ZnCl_2 ; *Arthrobacter* sialidase (Nakarai, Tokyo, Japan), specific for $\alpha(2,3/2,6/2,8)\text{NeuAc}$, 5 mU/mM in 50 mM ammonium acetate pH 5.0. The reaction was terminated by heating at 100°C for 2 min. The reaction mixture was centrifuged at 15,000 rpm for 20 min, in 0.2 mM low-binding hydrophilic polytetrafluoroethylene membrane Ultrafree™ centrifugal filter (Millipore, Bedford, MA) and the filtrate was applied to HPLC.

Analysis of N-glycan structures by three or two-dimensional HPLC mapping

The use of both normal-phase HPLC and reverse-phase HPLC to determine the structure of the complex N-glycans after removal of terminal galactose and outer-arm

fucose residues was carried out as described previously. Its elution position was compared with those of standard PA-oligosaccharides on the three or two-dimensional map.

Tissue preparation for histochemistry

ICR mice were perfused with 4% paraformaldehyde in PBS (pH 7.4), and then the brains were removed and postfixed in the same fixative for overnight at 4°C. Subsequently, samples were dehydrated in alcohol, embedded in paraffin and sectioned sagittally at 10 µm thickness.

Lectin histochemistry

Paraffin-embedded mouse sections were prepared at a thickness of 10 µm. Deparaffinized sections were incubated in xylene and graded series of ethanol. After washing with PBS and blocking with 5% BSA for 1 hr, sections were incubated overnight at 4°C with biotinylated-*Sambucus Nigra* (Elderberry) bark lectin (Vector Laboratory, Burlingame, CA) at 1:1000 dilution in PBS containing 0.1% TritonX-100

for overnight. After being rinsed with buffer, sections were incubated with avidin-biotinylated horseradish peroxidase (HRP) complex solution (Vectastain Elite ABC®; Vector Laboratories, Burlingame, CA) and were developed in 3' 3-diaminobenzidine (DAB) solution, or were incubated with fluoresce conjugated secondary anti-IgG followed by hematoxylin counterstaining, dehydrated and mounted.

Immunohistochemistry

Brain sections were blocked in TBS containing 5% BSA and 0.1% Triton X-100 for 30min. Using the same buffer solution, the sections were then incubated overnight at 4°C in primary antibodies with mouse monoclonal anti-GFAP (Sigma, USA) at 1:1000 dilution or with 1:1000 diluted rabbit polyclonal anti-Iba1 antibody (Wako, Japan) in PBS containing 0.1% TritonX-100. After 3 times wash in PBS, sections were incubated with corresponding fluorescent goat secondary IgG antiserum. Sections were coverslipped with PVA/DABCO (a mixture of glycerol, polyvinyl alcohol, Tris-HCl, diazabicyclooctane and H₂O) after 3 times wash in PBS.

SNA lectin affinity chromatography

SNA agarose beads (Vector Laboratory, Burlingame, CA) were packed into a 50×10 mm Assist mini-column. A 1-mL sample was applied to the SNA column after it had been equilibrated with buffer A, which consisted of 20 mM Tris-HCl (pH 7.5) containing 0.15 M NaCl, 1 mM MnCl₂, 1 mM CaCl₂. Unbound oligosaccharides were washed away with buffer A, and the bound sugar chains were eluted from the column with 0.1 M lactose in buffer A. After elution, I performed purification of oligosaccharides on 2D-HPLC for further analysis.

Results

Analysis of mouse cortical sialylated N-glycans

I first analyzed expression of sialylated N-glycans from mouse cortices according to the traditional method. N-glycans were extracted and pyridylaminated as described in Materials and Methods. I then applied the mixture onto a MonoQ column, which separates sugar chains according to their negative charge. I isolated fractions corresponding to neutral sugar chain-containing fraction (N), 1 sialic acid-containing fraction (S1), 2 sialic acids-containing fraction (S2) and so on (Fig. 2A). Sialic acid-containing sugar chains were treated with neuraminidase and then applied to a normal phase HPLC (Fig. 2B). N-glycan levels eluting from S4 fraction or fractions containing more sialic acids were very low compared to those from other fractions. More than 50% of total sugar chains were confirmed to be neutral sugar chains, which were mainly composed of oligomannose-type sugar chains, constituting 45.5% of total N-linked sugar chains in adult mouse cerebral cortex (Ishii *et al.* 2007). These highly abundant high mannose-type sugar chains (M5 to M9) can be detected on normal phase

HPLC chromatograms (Fig. 2B); however, other peaks are still incompletely separated and cannot be identified and quantified yet.

I thus fractionated the eluate from the normal phase HPLC into 30 fractions and applied fractions to reverse phase HPLC for further separation. I have improved the separation on normal phase HPLC as described in the Materials and Method and thus the number of fractions increased from 10 to 30, resulting in better separation (Fig.

3). Through this improvement I have identified three new sugar chains with relatively high abundance (more than 0.1% of total N-glycan content), which were not found in our previous analysis (Ishii *et al.* 2007) and are presented as X1 to X3 in Table 1.

Structures of these unidentified sugar chains were determined as described below. I obtained a two-dimensional map of three pyridylaminated (PA) N-linked sugar chains expressed in adult mouse brain with two indices consisting of mannose unit (MU) measured by normal phase HPLC and glucose unit (GU) measured by reverse-phase HPLC. I identified their structure by exoglycosidase digestion and MALDI/TOF/MS as following. Firstly, the molecular mass of these PA-sugar chains was analyzed by MALDI/TOF-MS. The monoisotopic mass of the MNa^+ ion of X1 PA-sugar chain

was 2034.76, indicating an isobaric monosaccharide composition of H5N4F2. The PA-sugar chain X1 showed an elution time in mannose units (MU) of 7.8 on normal phase HPLC and in glucose units (GU) of 10.8 on reverse phase HPLC. The sugar was susceptible to digestion with α 1,6-L-fucosidase (Fig. 4A (1)). In this case, one fucose residue was released, and the product was mapped to the position (GU 9.6, MU 7.1) on the two-dimensional map. Further digestion was performed with α 1,3/4-fucosidase (Fig. 4A (2)), resulting in the release of one fucose residue. This digested product was mapped to the position (GU 10.4, MU 6.6), which coeluted on reverse-phase HPLC with the standard PA-sugar chain, A2G2. The product after β 1,4-galactosidase digestion (Fig. 4A (3)) was further digested with α 1,6-fucosidase. The product (GU 12.3, MU 6.0) coeluted with the standard, A2G1(6)F. Thus the structure of PA-sugar chain X1 was determined to be A2G2Fo(6)F (Fig. 4A).

The monoisotopic mass of the MNa^+ ion of X2 PA-sugar chains was 2237.84, indicating the isobaric monosaccharide composition of H5N5F2. The PA-sugar chain X2 (GU 21.5, MU 7.9) was digested with β 1,4-galactosidase (Fig. 4B (3)). In this case, one galactose residue was released, and the product was mapped to the position (GU

20.8, MU 7.0) on the two-dimensional map. Further digestion was performed with α 1,3/4-fucosidase (Fig. 4B(2)), resulting in the release of one fucose residue. This digested product was mapped to the position (GU 22.3, MU 6.7), which coeluted on reverse-phase HPLC with the standard PA-sugar chain, Ga-BA-2. X2 was digested with α 1,3/4-fucosidase. The product (GU 23.0, MU 7.0) coeluted with the standard, G2-BA-2. Thus, the structure of the PA-sugar chain X2 was determined to be A2G2Fo(6)FB (Fig. 4B).

The monoisotopic mass of the MNa^+ ion of X3 PA-sugar chains was 1888.7, indicating an isobaric monosaccharide composition of H5N4F1. The PA-sugar chain X3 (GU 11.4, MU 7.0) was digested with *Xanthomonas manihotis* β 1,3-galactosidase (Fig. 4C (4)). In this case, one galactose residue was released, and the product was mapped to the position (GU 12.3, MU 6.0) on the two-dimensional map. Further digestion was performed with *Diplococcus pneumoniae* β -galactosidase (3), resulting in the release of one galactose residue. This digested product was mapped to the position (GU 11.4, MU 5.2), which coeluted on reverse-phase HPLC with the standard PA-sugar chain, A2G0F. The product after β 1,3 galactosidase digestion was further digested

with α 1,6-fucosidase. The product (GU 12.3, MU 6.0) coeluted with the standard, A2G1(6). Thus, the structure of PA sugar chain X3 was determined to be A2G1(6)G'1(3)F (Fig. 4C).

All other peaks whose content is over 0.1% of the total N-glycan content have been identified previously (Ishii *et al.* 2007). Since several chromatographic separation steps were employed to identify sugar chains, we could not reliably perform relative quantification of the sugar chains.

Thus I have developed a more practical approach for quantitative analysis of sialylated N-glycans. I treated the pyridylaminated sugar chain mixture with neuraminidase, then applied to MonoQ HPLC and obtained the flow through fraction. This fraction contains neutral sugar chains and desialylated sugar chains (N+D fraction). Figure 5-a shows a differential display of normal phase HPLC pattern obtained from N+D fraction (solid line) and N fraction (broken line). The amount of sialylated sugar chains can be estimated by comparing the area of each peak obtained from N fraction with that from N+D fraction. However, the separation was insufficient, thus I further applied these fractions to the reverse phase HPLC. Figure 5-b shows a reverse phase

HPLC chromatogram of a fraction indicated by a bar in Fig. 5-a. Now the sialylated component of each sugar chain is visible. For example, A2G2 (indicated by an arrow) was detected only in the N+D fraction, but not in the N fraction. This indicates that A2G2 was completely sialylated. On the other hand, a sugar chain indicated by an arrowhead is equally abundant in N and N+D fractions, indicating that this sugar chain is not sialylated at all. Most sialylated N-glycans present in the mouse cortex were systematically separated and quantified using this system (Table 2, lanes C ^{α 2,3/6/8}). From Table 2 it is clear that the LewisX epitope present in the mouse cortex from any developmental stage is not sialylated. Thus there are no sialyl LewisX moieties in mouse cortices.

Analysis of the linkage of sialic acid residue on N-glycans

To determine the linkage of sialic acid residue on N-glycans, I performed an analysis using Newcastle Disease Virus sialidase [specific for α 2,3(8)NeuAc]. Pyridylaminated sugar chains were treated with α 2,3-sialidase in place of neuraminidase and analyzed as described before through MonoQ HPLC to reverse

phase HPLC. Examples of HPLC profiles I used for further calculation are shown in Fig. 6. Quantification of α 2,3-sialidase-sensitive proportion of major sialylated N-glycans is presented in Table 2. When all the sialic acid residues are connected to N-glycans via an α 2,3-linkage, the neuraminidase sensitive portion ($C^{\alpha 2,3/6/8}$ value) and α 2,3-sialidase sensitive portion ($C^{\alpha 2,3}$ value) should be the same. It is evident that N-glycans with type 1 antennary always harbor α 2,3-sialidase resistant sialic acid residues, while N-glycans with type 2 antennary in the adult and in embryonic day 12 (E12) cortices mostly harbor α 2,3-sialidase sensitive sialic acid residues. This is in good agreement with the previous finding that most of the sialic acid residues in the brain are connected via α 2,3-linkages (Zamze *et al.* 1998). However, around birth (E16, post-natal day 0 (P0) and P7) some portion of sialic acid residues become α 2,3-sialidase resistant (see A2G2 and A2G2F).

I next determined how many α 2,3-sialidase resistant sialic acid residues are present in each of the N-glycan contains. The cortical PA-sugar chain mixture was first treated with α 2,3-sialidase and then fractionated on MonoQ HPLC followed by neuraminidase treatment, and analyzed on normal and reverse phase HPLC. In Table

3 N-glycans recovered from S1 fraction and those from S2 fraction are listed. I could not detect any N-glycans in S3 or S4 fractions.

Identification of a novel structure containing α 2,6-sialic acid residue in the mouse brain

I determined the structure of N-glycans containing α 2,3-sialidase resistant sialic acid residues. I started from analyzing the adult cortex because it only contains α 2,3-sialidase resistant N-glycans with type 1 antennary (Tables 2 and 3). Two major peaks that were resistant to α 2,3-sialidase treatment were A2G'2F and A2G1(6)G'1(3)F.

Both sugar chains were recovered mainly from the S2 fraction (Table 1), thus both of them contain two sialic acid residues. After α 2,3-sialidase treatment, A2G'2F was recovered equally from the S1 and S2 fractions (Table 3 and arrows in Fig. 7), indicating that half of the A2G'2F has two α 2,3-sialidase resistant sialic acids whilst the other half contains one resistant and one sensitive sialic acid residue. A2G1(6)G'(3)1F was mainly recovered from the S1 fraction (Table 3 and arrowhead in Fig. 7), thus it has

one sialic acid residue resistant to and one sensitive to α 2,3-sialidase.

The next step was to determine at which position the sialic acid residues are attached. I focused on A2G'2F with two α 2,3-sialidase resistant sialic acids because I wanted to determine the structure of α 2,3-sialidase resistant sialic acid-containing N-glycans. I decided to isolate A2G'2F in its sialylated (native) form. The PA-sugar chain mixture extracted from mouse cortex was subjected to MonoQ HPLC and the S2 fraction was recovered (Fig. 8A-a). Sugar chains in this fraction were treated with α 2,3-sialidase, subjected to MonoQ HPLC and the S2 fraction was collected again (Fig. 8A-b). This fraction should only contain sugar chains that have two α 2,3-sialidase resistant sialic acid residues. This fraction was separated by reverse phase HPLC in the presence of triethylamine (Fig. 8B). There were 4 major peaks in this fraction. Each peak was collected, treated with neuraminidase, and analyzed on normal and reverse phase HPLC. Peak 3 in Fig. 8B generated A2G'2F, thus this sugar chain is the one I desired. The peak 3 was collected and then digested with β 1,3-galactosidase to know whether the sialic acid is attached to the terminal galactose residue or not. After the enzyme reaction, the elution time for the sugar chain on reverse phase HPLC with

triethylamine changed, indicating that at least one galactose residue was removed (Fig. 8C). This product was analyzed by MonoQ HPLC and was indicated to contain 2 sialic acid residues (data not shown). After neuraminidase treatment the galactosidase-reaction product was analyzed by 2D-HPLC mapping and was identical to A2G0F (Fig. 9). These results demonstrate that sialic acids were not attached to the terminal galactose residues of the sialylated N-glycan. As far as we know, the only possible attachment site of sialic acids other than galactose is the 6th position of GlcNAc residue. Thus, I propose the structure to be the one presented in Fig. 6.

As far as I know, this is the first report on identification of branched α 2,6-sialylated N-glycans without terminal galactose sialylation.

N-Glycans containing NeuAc α 2,6Gal β 1,4GlcNAc epitope are temporarily expressed during development in the mouse cerebral cortex.

Next I investigated the structure of N-glycans containing the sialylated Gal β 1,4GlcNAc structure that are resistant to α 2,3-sialidase treatment and are temporarily detected in the cortex (Table 2). I hypothesized the structure to be an α 2,6-linked sialylated

N-glycans containing [Neu5Ac α 2,6Gal β 1,4GlcNAc] structure. To confirm these α 2,3-sialidase resistant N-glycans indeed contain a Neu5Ac α 2,6Gal β 1,4GlcNAc structure, SNA lectin affinity chromatography was performed. The initial PA-sugar chain mixture was applied to the SNA lectin column and the adsorbed fraction was further subjected to MonoQ HPLC analysis. Most of the sugar chains were recovered in the S1 and S2 fractions (data not shown). After neuraminidase treatment, the structure of the sugar chains in these fractions was determined by 2-D HPLC analyses, which are shown in Figure 10. They were all type 2 sugar chains containing Gal β 1,4GlcNAc structure. These results indicated that the Neu5Ac α 2,6Gal β 1,4GlcNAc structure appears temporarily in the mouse cortex during development. This result also excludes the presence of the type 1 (Gal β 1,3GlcNAc) structure harboring sialic acid residues attached to the galactose residue via an α 2,6-linkage (Neu5Ac α 2,6Gal β 1,3GlcNAc).

The sialylated N-glycans expressed in mouse cortices during development listed in Table 2 are categorized by their sialic acid linkage type and are shown in figure 11. It is clear that the expression of sialyl N-glycans is dynamically changing during

development. Type 2 N-glycans containing sialic acid attached to the terminal galactose residue via α 2,3 linkage are most abundantly expressed in the mouse cortex throughout development, while those containing sialic acid attached to galactose via α 2,6 linkage are temporarily expressed reaching their maximum level around birth. N-glycans with the new sialic acid-containing structure [Gal β 1,3(NeuA5 α 2,6)GlcNAc-] are absent or present in very low amounts at E12, but increase their expression level during development, reaching nearly 2% of the total N-glycan level in the adult.

Localization of sialylated oligosaccharides

To study the localization of sialylated oligosaccharides, immunostaining and lectin histochemistry were performed in paraffin-embedded developing and adult cortices using *Maackia amurensis* (MAA, specific for NeuAc α 2,3Gal) and *Sambucus nigra* (SNA, specific for NeuAc α 2,6Gal β 1,4GlcNAc-) lectins. Since paraffin preparation is devoid of lipids, including glycolipids, only glycoprotein should be detected by the lectin staining. The localization of new type of sialylated N-glycans I found in this

study could not be investigated because the lectin that binds to this structure is not known yet.

In the MAA lectin histochemical image, many cells were stained throughout the cortex, and it was not possible to identify the cell type (Fig. 12). Thus, NeuAc α 2,3Gal structure seems to be ubiquitously expressed in the mouse cortex.

On the other hand, by the SNA lectin histchemistry, some epithelial cells and choroids plexus cells were strongly reactive during all the stages in mouse cerebral cortex. These SNA staining was abolished by preincubation with excess amount of neuraminidase (data not shown). SNA lectin positive cells were also found in the SVZ area in P0 (Fig. 13) and P7 (Fig. 14, A and B) cortices, while no such staining was found in E12 or 12w cortices. This temporal appearance of SNA lectin positive cells matches well with the temporal expression of NeuAc α 2,6Gal β 1,4GlcNAc-carrying N-glycans (Table 2).

I then identified the cell type of SNA lectin positive cells. Their nuclei were small, so they were likely to be non-neuronal cells (Fig. 14F). The SNA positive cells, which were present in the SVZ, did not express GFAP, an astrocyte marker, in P7

mouse cerebral cortex (Fig. 14E and F), but expressed microglia marker Iba1 (Fig. 14 B-D). Some of the Iba1 positive cells that were present in the grey matter were not labeled with the SNA lectin. The SNA positive cells in the SVZ of P0 cortex were also costained with Iba1 (Fig. 13 E-G). These cells seem to be ameboidmicroglia as judged from their round morphology. SNA lectin positive cells might be immature microglia or cells of the blood corpuscle origin, such as macrophage, that entered brain from the blood vessel.

Discussion

Characterization of major sialylated N-glycans derived from developing and adult cerebral cortices.

Expression pattern of neutral and asialo-sugar chains from brain were analyzed and characterized as described (Zamze *et al.* 1998; Chen *et al.* 1998, Ishii *et al.* 2007). In this report, I analyzed major sialylated N-linked oligosaccharides expressed in the developing mouse cerebral cortices by the high resolution HPLC system and determined their structure. It is essential to determine the entire structure of sialylated sugar chain, including all the linkage between sugar residues, to understand roles played by siglecs and sialylated sugar chains. It is also important to know their expression levels during development. Previous study by Zamze *et al.* (1998) reported comprehensive analysis of sialylated N-glycans in the adult rat brain, however, several crucial points were missing. 1) Linkage of sialic acid attached to each of N-glycan was not analyzed. 2) They analyzed only adult brains, but did not analyze developing brains. 3) Quantification of N-glycans was based on MALDI-TOF massspectrometrical analysis,

thus expression level of different sugar chains cannot be compared with each other. To overcome these problems, I established a new method to analyze sialic acid-containing N-linked sugar chains in tissue samples, and systematically analyzed expression level and linkage of sialylated N-glycans in developing and adult mouse cerebral cortices. We may be able to analyze other acidic oligosaccharides (such as sulfonated sugar chains) by this analyzing system. I also used neuraminidase and α 2,3-sialidase to determine the linkage of sialic acid attachment. Through my analysis the entire structure and the expression level of all the N-glycans whose content exceeds 0.1 % of total N-glycan content have been elucidated.

I found mainly three types of linkage between sialic acid and N-glycans. 1)

NeuAc α 2,3Gal β 1,4GlcNAc-, 2) NeuAc α 2,6Gal β 1,4GlcNAc-, 3)

Gal β 1,3(NeuAc α 2,6)GlcNAc- (Fig. 11).

The first structure was the most abundant throughout the development, which is in good accordance with the previous finding using adult rat brain (Zamze *et al.* 1998). This structure is formed by ST3Gal enzyme family (ST3Gal I, ST3Gal II, ST3Gal III, ST3Gal IV, ST3Gal V and ST3Gal VI). Among these, ST3Gal IV and

ST3GalVI show preference toward type 2 sugar chains and thus these enzymes may be responsible for synthesis of the first structure. However, in situ hybridization analyses (Matsushashi *et al.* 2003) or our cDNA macroarray analysis (Ishii *et al.* 2007) revealed very low level of expression of these genes in adult mouse cerebral cortex. Therefore, the enzyme responsible for its synthesis is currently unknown.

The second structure was temporary expressed during development and was very low in the adult. Low expression in the adult again agrees well with the previous finding (Zamze *et al.* 1998), but temporal expression is a new finding. I also found that α 2,6-sialylated N-glycans attached to terminal galactose were mainly synthesized in microglia at around birth (Fig. 13 and 14). As far as I know, terminal α 2,6-sialylation of complex-type containing Gal β 1,4GlcNAc- residue on N-linked oligosaccharides is dependent on the expression of ST6Gal I or II. Expression of ST6Gal I is developmentally regulated, tissue-specific, and involved in the regulation of a number of important cell processes (Hamamoto *et al.* 2002). However, only the expression of ST6Gal II was detected in the adult mouse brain by Northern blot analysis (Takashima *et al.* 2002), although it is possible that the other member of ST6Gal family

or other enzymes are temporarily expressed in microglia specifically at these early stages. Interestingly, both ST6Gal I and II are detected at these stages in our cDNA macroarray analysis (Ishii *et al.* 2007).

Influenza viruses have been associated with a broad spectrum of CNS complications extending from acute encephalitis/encephalopathy to neuropsychiatric disorders (Mori and Kimura, 2001). Interestingly, NeuAc α 2,6Gal- structure forms a receptor for human influenza virus (Baum and Paulson 1990; Guo *et al.* 2007) and thus its temporal expression in neonatal mouse brain may become important to understand the reason for higher incidence of influenzal encephalitis among younger people compared to the adult if the same happens in the human brain

The third structure is novel. In rat brain the same back bone (A2G'2F) harbors disialyl LewisC (NeuAc α 2,3Gal β 1,3(NeuAc α 2,6)GlcNAc) epitope and mainly bears 4 sialic acid residues (Zamze *et al.* 1998). I initially suspected that the sialic acid residue attached to the galactose residue within the LewisC epitope on A2G'2F had been artificially removed during our N-glycan preparation procedure. Therefore, I started from a standard PA-sugar chain containing the disialyl LewisC epitope (TaKaRa,

PA-sugar chain 025) and completely followed my preparation procedure from hydrazinolysis to pyridylation. The disialyl LewisC epitope was recovered in a totally intact form (data not shown), thus this new structure is not an artifact. Moreover, I believe that A2G1Fo(6)G'1(3)F with one α 2,3-sialidase resistant and one sensitive sialic acids (Table 1 and 3) has been recovered as intact disialyl LewisC-containing N-glycan. There are no direct evidence for this, but I have never detected sialic acid connected to the LewisX epitope in the mouse cortex (Table 2), thus it is reasonable to speculate that the Man(6) branch with LewisX epitope has no sialic acid attached, while the Man(3) branch with type 1 galactose structure harbors two sialic acid residues forming disialyl LewisC epitope. Therefore, it seems that there is a great difference in the N-glycan structure between rat and mouse cortices on type 1 antennary. It must be investigated whether siglecs which bind to disialyl LewisC epitope or monosialyl LewisC epitope are distinct from each other or not.

Biosynthetic pathway of this novel sialyl structure on N-glycan is interesting.

There are two possibilities. 1) A synthetic route similar to disialyl-LewisC structure pathway can be proposed. Initially, terminal galactose on type 1 sugar chain

(Gal β 1,3GlcNAc-) might be α 2,3-sialylated by ST3GalIII, because mouse ST3GalIII has a strong preference for Gal β 1,3GlcNAc/GalNAc- residue over Gal β 1,4GlcNAc, as reported for rat and human ST3GalIII (Tsuji 1996). Next the ST6GalNAc family or unidentified α 2,6-sialyltransferase enzyme adds the sialic acid to GlcNAc, recognizing this α 2,3-sialylated form of sugar chain. As a result, sugar chain containing disialyl-Lewis C residues on N-glycan will be synthesized via pathway indicated in Fig. 15 (dotted square). The α 2,3-linkage sialic acid attached to terminal galactose of N-linked sugar chain will be removed to become this novel structure. However, if this is true, there must be an unidentified sialidase with high specificity toward α 2,3-linkage sialic acid on disialyl-Lewis C residues because I observed very few type 2 sugar chains with a free (non-sialylated) galactose residue.

2) There might be a route to synthesize this structure by directly attaching sialic acid to GlcNAc on type 1 sugar chain (Fig. 15, indicated by a vertical arrow). Even in this case, such an enzyme activity has not been found yet.

Biosynthetic pathway for sialylated N-glycans in mouse cortices

I have never detected NeuAc α 2,6Gal β 1,3GlcNAc- structure. There are two known enzymes that adds sialic acid residue to the galactose moiety via α 2,6 linkage (ST6Gal I and II). These enzymes do not utilize type 1 antennary as a substrate (Hamamoto *et al.* 1993; Hamamoto *et al.* 2002; Takashima *et al.* 2003). I also repeated this experiment using purified enzymes and A2G'2F as a substrate in vitro with the help of Prof. Shuichi Tsuji and Dr. Yoshie Takaki (Tokai University) but we were not able to detect any reaction products, while A2G2F served as a good substrate (data not shown). Taken all together, there seem to be several important steps in biosynthetic pathway of sialylated N-glycans in mouse cortices that are critical in deciding which types of structure an antennary bears.

First branching point is the attachment of Gal to GlcNAc (Fig. 15, step (1)).

In the mouse brain, a large proportion of N-glycans ends their synthesis at this step without further addition of Gal (Ishii *et al.*, 2007). Majority of N-glycans attach Gal via β 1,4 linkage, however, once the Gal residue is attached via β 1,3 linkage forming type 1 antennary, most of the branches become LewisC type.

Second branching point appears on type 2 antennary at step (2) (Fig. 15). At

this point only a small portion of N-glycans stop biosynthesis with free Gal β 1,4GlcNAc structure, but proceed further to adding either Fuc to GlcNAc or NeuAc to Gal. When the Fuc residue is attached, it serves like a capping structure, preventing addition of sialic acid. The fucose free structure mainly adds NeuAc via α 2,3 linkage, but occasionally (temporary during development) it is modified via α 2,6 linkage.

Ameboidmicroglia is stained with SNA lectin.

To determine the cell type of the SNA positive cells, immunostaining was performed using various antibodies (Fig. 12 and 13). It has been reported that choroid plexus epithelial cells and ependymal cells reacted with SNA and arachnoid cells, pia matter, astrocyte and oligodendrocytes did not react with SNA, in human and rat CNS (Kaneko *et al.* 1995). I found that Iba 1 positive microglial cells are temporary stained with SNA lectin. There are four lectins (*Abrus precatorius* (APA), *Maackia amurensis* (MAA), *Momordica charantia* (MCA) and *Sambucus nigra* (SNA)) which have been used to identify the microglial cells (Zambenedetti *et al.* 1998). The specificity of SNA against microglia was previously described, by Mann *et al.* (1992) in Down's

syndrome brains and by Lutsik *et al.* (1991), who reported an increase in microglial cells in meningoencephalitis cases with a large production of SNA positive perivascular cells. Mann *et al.* (1992) reported that SNA in tissues from non-demented elderly individuals detects only occasionally microglia, suggesting that SNA most likely detects only subset of microglia probably those that have been activated. The SNA positive microglial cells that I detected around birth in the SVZ may form a subtype of microglia and have specific function during development

Conclusion

In the present study, I characterized the sialylated N-glycans expressed in mouse cortex during development, comprehensively. The present result will form important basis for elucidating the regulatory mechanism and physiological significance of sialylated N-linked sugar chains in the CNS during development.

Acknowledgments

I wish to express my gratitude to many people in completing my thesis and research during these four years.

Prof. K. Ikenaka, my supervisor and head of Division of Neurobiology and Bioinformatics, National Institute of Physiological Sciences, National Institutes of Natural Sciences. I would like to thank him specially for introducing me such an exciting theme as glycobiology and for his valuable guidance throughout this study.

Dr. S. Hitoshi. I would like to thank him for making a number of helpful suggestions.

Dr. K. Ono. I would like to thank him for teaching me immunohistochemistry and lectin histochemistry.

Dr. T. Toda, Research Team for Molecular Biomarkers, Tokyo Metropolitan Institute of

Gerontogy for instructing me MALDI/TOF-MS analysis.

Dr. M. Higashi and Mr. G. Yamada. I wish to thank them for various help and valuable advices.

Ms. I. Ito. I would like to thank her for technical assistance on HPLC analysis.

MALDI/TOF-MS analysis was performed in the NIBB Center for Analytical Instruments, National Institutes of Natural Sciences, Okazaki, Aichi 444-8585, Japan

References

Attrill, H., Takazawa, H., Witt, S., Kelm, S., Isecke, R., Brossmer, R., Ando, T., Ishida, H., Kiso, M., Crocker, P. and Aalten, D. (2006) The structure of siglec-7 in complex with sialosides: leads for rational structure-based inhibitor design. *Biochem. J.*, **397**, 271-278.

Baum, L. G. and Paulson, J. C. (1990) Sialyloligosaccharides of the respiratory epithelium in the selection of human influenza virus receptor specificity. *Acta. Histochem. Suppl.* **40**, 35-38.

Chen, Y. J., Wing, D. R., Guile, G. R., Dwek, R. A., Harvey, D. J., and Zamze, S. (1998) Neutral N-glycans in adult rat brain tissue: Complete characterization reveals fucosylated hybrid and complex structures. *Eur. J. Biochem.*, **251**, 691-703.

Crocker, P.R. (2002) Siglecs: sialic-acid-binding immunoglobulin-like lectins in cell-cell

interactions and signaling. *Curr. Opin. Struct. Biol.* **12**, 609-615.

Fischer, E., and Brossmer, R. (1995) Sialic acid-binding lectins: submolecular specificity and interaction with sialoglycoproteins and tumour cells. *Glycoconj. J.*, **12**, 707-713.

Fujimoto, I., Menon, K. K., Otake, Y., Tanaka, F., Wada, H., Takahashi, H., Tsuji, S., Natsuka, S., Nakakita, S., Hase, S., Ikenaka, K. (1999) Systematic analysis of N-linked sugar chains from whole tissue employing partial automation. *Anal Biochem.*, **267**, 336-343.

Guo, C. T., Takahashi, N., Yagi, H., Kato, K., Takahashi, T., Yi, S. Q., Chen, Y., Ito, T., Otsuki, K., Kida, H., Kawaoka, Y., Hidari, K. I-P. J., Miyamoto, D., Suzuki, T., Suzuki, Y. (2007) The quail and chicken intestine have sialyl-galactose sugar chains responsible for the binding of influenza A viruses to human type receptors. *Glycobiology.* **17**, 713-724.

Hakomori, S. (1981) Glycosphingolipids in cellular interactions, differentiation and oncogenesis. *Annu. Rev. Biochem.* **50**, 733-764.

Hamamoto, T., Kawasaki, M., Kurosawa, N., Nakaoka, T., Lee, Y. -C., and Tsuji, S. (1993) Two-step single primer-mediated polymerase chain reaction. Application to cloning of putative mouse, β -galactoside α 2,6-sialyltransferase cDNA. *Bioorg. Med. Chem.* **1**, 141-145.

Hamamoto, T. and Tsuji, S. (2002) ST6Gal-1 in *Handbook of Glycosyltransferases and Related Genes* (Taniguchi, N., Honke, K., and Fukuda, M, eds) pp. 295-300, Springer-Verlag, Tokyo, Japan.

Hase, S., Ikenaka, T., and Matsushima, Y. (1981) A high sensitive method for analysis of sugar moieties of glycoproteins by fluorescence labeling. *J Biochem.*, **90**, 407-414.

Hase, S., Natsuka, S., Oku, H., and Ikenaka, T. (1987) Identification method for twelve

oligomannose-type sugar chains though to be processing intermediates of glycoproteins.

Anal Biochem., **167**, 321-326.

Hase, S. (1994) High performance liquid chromatography of pyridylaminated saccharides.

Methods Enzymol., **230**, 225-237.

Hase, S., Ikenaka, K., Mikoshiba, K., and Ikenaka, T. (1998) Analysis of tissue glycoprotein sugar chains by two-dimensional high-performance liquid chromatographic mapping. *J Chromatogr.*, **434**, 51-60.

Ishii, A., Ikeda, T., Hitoshi, S., Fujimoto, I., Torii, T., Sakuma, K., Nakakita, S., Hase, S., and Ikenaka, K. (2007) Developmental changes in the expression of glycogenes and the content of N-glycans in the mouse cerebral cortex. *Glycobiology.*, **17**, 261-276.

Kaneko, Y., Yamamoto, H., Kersey, D., Colley, K., Leestma, J., and Moskal, J. (1996)

The expression of Gal β 1,4GlcNAc α 2,6 sialyltransferase and α 2,6-linked

sialoglycoconjugates in human brain tumors. *Acta Neuropathol.*, **91**, 284-292.

Kleene, R. and Schachner, M. (2004) Glycans and neural cell interactions. *Nature Rev. Neurosci.*, **5**, 195-208.

Lau, K. S., Partridge, E. A. Grigorian, A., Silvescu, C. I., Reinhold, V. N., Demetriou, M., Dennis, J. W. (2007) Complex N-glycan number and degree of branching cooperate to regulate cell proliferation and differentiation. *Cell*, **129**, 123-134.

Lutsik, B. D., Iashchewko, a. M., and Lutsik, A. D. (1991) Lektinoperoksidaznye markery mikroglia v parafinovykh srezakh. *Arkhiv Patologii.* **53**, 60-63.

Mann, D. M. A., Younis, N., Jones, D., and Stoddart, R. W. (1992) The time course of pathological events in Dawn's Syndrome with particular reference to the involvement of microglial cells and deposits of β /A4. *Neurodegeneration.* **1**, 201-215.

Matsubishi, H., Horii, Y., and Kato, K. (2003) Region-specific and epileptogenic-dependent expression of six subtypes of α 2,3-sialyltransferase in the adult mouse brain. *J. Neurochem.*, 84 : 53-66.

Miyoshi, E., Nishikawa, A., Ihara, Y., Gu, J., Sugiyama, T., Hayashi, N., Fusamoto, H., Kamada, T., Taniguchi, N. (1993) N-acetylglucosaminyltransferase III and V messenger RNA levels in LEC rats during hepatocarcinogenesis. *Cancer Res.*, **53**, 3899-3902.

Mori, I., and Kimura, Y. (2001) Neuropathogenesis of influenza virus infection in mice. *Microbes Infect.* **3**, 475-479.

Ngamukote, S., Yanagisawa, M., Ariga, T., Ando, S., and Yu, R. (2007) Developmental changes of glycosphingolipids and expression of glycogenes in mouse brains. *J. Neurochem.*, **103**, 2327-2341.

Ohtsubo, K., and Marth, J. D. (2006) Glycosylation in cellular mechanisms of health and disease. *Cell*, **126**, 855-867.

Schachner, M. and Bartsch, U. (2000) Multiple functions of the myelin-associated glycoprotein MAG (siglec-4a) in formation and maintenance of myelin. *Glia*, **29**, 154–165.

Takashima, S., Tsuji, S., Tsujimoto, M. (2003) Comparison of the enzymatic properties of mouse β -Galactoside α 2,6-sialyltransferases, ST6Gal I and II. *J. Biochem.* **134**, 287-296.

Tanabe, K and Ikenaka, K. (2006) In-column removal of hydrazine and N-acetylation of oligosaccharides released by hydrazinolysis. *Anal Biochem.*, **348**, 324-326.

Tsuji, S. (1996) Molecular cloning and functional analysis of sialyltransferases. *J. Biochem.* **120**, 1-13.

Vyas, A., Blixt, O., Pauson, J., and Schnaar, R. (2005) Potent glycan inhibitors of myelin-associated glycoprotein enhance axon outgrowth *in vitro*. *J.Biol.Chem.*, **280**, 16305-16310.

Zamze, S., Harvey, D.J., Chen, Y., Guile, G.R., Dwek, R.A., and Wing, D.R. (1998) Sialylated N-glycans in adult rat brain tissue—a widespread distribution of disialylated antennae in complex and hybrid structures. *Eur. J. Biochem.*, **258**, 243-270.

Zambenedetti, P., Giordano, R., and Zatta, P. (1998) Histochemical localization of glycoconjugates on microglial cells in Alzheimer's disease brain samples by using *Abrus precatorius*, *Maackia amurensis*, *Momordica charantia*, and *Sambucus nigra* lectins. *Experimental neurology*. **153**, 167-171.

Figure legends

Figure 1: Outline of the general strategy employed in this study

Tissue samples were homogenized with nine-fold volume acetone, and the precipitates were lyophilized. The amount of samples for hydrazinolysis was 2 mg. Samples were hydrazinolysed to release sugar chains and then N-acetylated. Removal of excess hydrazine and re-N-acetylation of sugar chains were performed manually on the graphite carbon column (Tanabe and Ikenaka, 2006). Sugar chains were converted to pyridylaminated (PA) derivatives manually. Excess reagents were removed by a cellulose column. The PA-sugar chains, containing both sialylated and neutral components, were digested by neuraminidase for further analysis (1) and α 2,3-sialic acid on N-glycans were digested by α 2,3-sialidase (3). The flow through fraction on MonoQ column HPLC containing desialylated and neutral N-glycans was collected and were analyzed by two-dimensional HPLC.

Figure 2: Analysis of sialylated N-glycans using HPLC system

(A) MonoQ HPLC chromatogram from 12w mouse cortex. N, S1, S2, S3 and S4 indicate the elution position of neutral, monosialo, disialo, trisialo and tetrasialo-PA oligosaccharides, respectively.

(B) Normal-phase chromatograms of neutral and desialylated PA-sugar chains from the P0 mouse cerebral cortex. After fractionation on a MonoQ column, each fraction was analyzed by normal-phase HPLC. N, S1 S2, S3 and S4 indicate the fractions from MonoQ HPLC that contain neutral-, mono-, di-, tri-, and tetra-sialyl oligosaccharides, respectively. M5-M9 indicate high-mannose type sugar chains.

Figure 3: Excellent separation of PA-sugar chains achieved on normal-phase HPLC

The PA-sugar chains were fractionated into 30 fractions on normal phase HPLC referring to high mannose type standards. These fractions were further separated by a Develosil C30-UG-5 column reverse-phase HPLC.

Figure 4: Schemes showing two-dimensional mapping of desialylated N-glycans

after exoglycosidase treatment

On this map, the horizontal and vertical axes correspond to GU (reverse phase HPLC) and MU (normal phase HPLC), respectively. Trajectories for enzymatic digestion were indicated by arrows with solid lines. The number of the plotted points indicates the oligosaccharide structures. The nomenclature of the structures is shown in footnote. Composition: H = hexose, N = GlcNAc, F = Fucose. Enzymes: bovine kidney α 1,6-fucosidase (1), α 1,3/4-L-Fucosidase (2), *Xanthomonas manihotis* β 1,3-galactosidase (3) and *Diplococcus pneumoniae* β -galactosidase (4) .

Figure 5: A simple method to quantify the sialylated portion of N-glycans

Neutral and asialo N-glycans, which were treated with neuraminidase, were separated and fractionated by MonoQ HPLC. Fractions were then analyzed by normal-phase HPLC (a) and a fraction indicated by a bar was collected. This fraction was separated by reverse-phase chromatography for further analysis (b). Black line indicates the chromatogram of neutral and desialylated PA-oligosaccharides derived from P0 mouse brain and gray line indicates that of neutral sugar chains. From the composite image

of two chromatograms sialylated sugar chains can be calculated as a difference in the peak area. Arrow indicates the elution position of A2G2, arrowhead indicate the elution position of A1G1FoFB.

Figure 6: Quantification of α 2,3-sialidase sensitive portion of sialylated N-glycans

PA-sugar chains were obtained from P0, P7 or 12w mouse cortices and were treated with neuraminidase or α 2,3-sialidase followed by MonoQ HPLC fractionation. The flow through fraction was applied to normal-phase HPLC and each fraction was further applied to reverse phase HPLC. Figures show reverse-phase HPLC chromatogram of a fraction obtained through normal phase HPLC. Black line indicates the chromatogram of neutral and desialylated PA-oligosaccharides and gray line indicates that of neutral sugar chains. From the composite image of two chromatograms neuraminidase sensitive or α 2,3-sialidase sensitive portion of sugar chains can be calculated as a difference in the peak area. Arrow indicates elution position of A2G2.

Figure 7: Estimation of the number of α 2,3-sialic acid attached to the sugar chains

Figures show reverse phase HPLC chromatogram of neutral and acidic fractions (S1-S4), which had been separated by MonoQ HPLC after α 2,3-specific sialidase treatment, followed by neuraminidase treatment. N, S1 and S2 indicate the fractions that contain neutral, mono- and di-sialyl- oligosaccharides, respectively. Arrow indicates elution position of A2G'2F and arrowhead indicates elution position of A2G1(6)G'1(3)F.

Figure 8. Isolation of unidentified α 2,3 sialidase resistant sialylated N-glycan

(A) Separation by MonoQ HPLC of N-glycans from 12w mouse brain. N, S1-S4 indicate the elution position of neutral, monosialo, disialo, trisialo and tetrasialo PA-N-glycans, respectively. N-glycans derived from 12w cerebral cortex were applied to MonoQ HPLC (a) and S2 fraction (indicated by oblique lines) was collected.

(b) After α 2,3-sialidase treatment the fraction was applied to MonoQ HPLC again.

(B) S2 fraction was applied onto ODS column and the fraction indicated by oblique

lines was collected.

(C) N-glycans in this fraction was treated with β 1,3-galactosidase and applied onto ODS column again. Peak 5 was collected for further analysis.

Figure 9: Proposed structure of unidentified sialylated N-glycan

Presumed structure of N-glycan that was isolated as in Fig. 8B is shown at the upper panel. After β 1,3-galactosidase treatment, galactose-removed sugar chain was collected (Fig. 8C, middle panel), which still harbored two sialic acids as determined by MonoQ HPLC (data not shown). Finally, this degalactosylated sugar chain was treated with neuraminidase and its structure was determined by the 2D-HPLC, which turned out to be A2G0F (lower panel).

Figure 10: Reverse-phase chromatogram of PA-sugar chain after SNA lectin affinity chromatography

PA-sugar chains derived from P0 mouse cortex were prepared according to the protocol, and applied to a SNA lectin column. Eluted sample was subjected to MonoQ HPLC

and S1-2 fraction was recovered after SNA lectin chromatography. Each acidic fraction was separated by normal phase HPLC after neuraminidase treatment. Fractionated each fraction was further applied to reverse phase HPLC. a-d indicate elution position of identified desialylated N-glycans. α 2,6 mono-sialylated A2G2 (a), Ga-BA-2 (b), Gb-BA-2 (c) and A2G2F (d). α 2,6 disialylated A2G2 (e), A2G2F (f), G2-BA-2 (g).

Figure 11: Dynamic change in the linkage and levels of sialylated N-glycan in mouse cortices during development

Relative abundance of sialylated N-linked sugar chains derived from developing and adult cerebral cortex (E12, E16, P0, P7 and 12 weeks) containing ■ , NeuAc α 2-3Gal β 1-4GlcNAc; ▲ , NeuAc α 2-6Gal β 1-4GlcNAc; × , Gal β 1-3(NeuAc α 2-6) GlcNAc is shown.

Figure 12: MMA lectin staining on mouse brain sections

Sagittal paraffin brain sections from 12w mouse was reacted with the *Maackia amurensis*. lectin (MMA), and detected by fluorescence. Green signal indicates MMA lectin positive cells (green; A and B) and superimposed with the Hoechst33258 for nuclear staining (blue) to produce the mixed image (B). Scale bars, 50 μ m.

Figure 13: SNA lectin staining on P0 mouse brain sections

Sagittal paraffin brain sections from P0 mouse was reacted with the *Sambucus nigra L.* lectin (SNA), and detected by DAB-staining (A, B) or by fluorescence (C-G). SNA lectin positive signal (green, E) was superimposed with the Iba1-specific signal (red, F) to produce the mixed image (G). Scale bars, 100 μ m.

Figure 14: SNA lectin staining on P7 mouse brain sections

Sagittal paraffin brain sections from P7 mouse was reacted with the *Sambucus nigra L.* lectin (SNA), and detected by fluorescence (A, B). SNA lectin positive signal (green) was superimposed with the Iba1-specific signal (red; C) to produce the mixed image (D). SNA positive cells (green), which localized in the SVZ, did not express GFAP (glial

fibrillary acidic protein)(red; E, F), an astrocyte marker, in P7 mouse cerebral cortex, but colocalized with a microglia marker, Iba1. Scale bars, 100 μ m.

Figure 15: Biosynthetic pathway for sialylated N-glycans in mouse cortices

Synthetic pathways in mouse cortices are indicated by black arrows. Identified sialylated and fucosylated N-glycans were enclosed in black square. (1) indicates first branching point, that is attachment of Gal to the terminal GlcNAc. (2) indicates second branching point on type 2 oligosaccharide; two types of sialylation products or fucosylation (LewisX synthesis) can be formed.

Figure 1

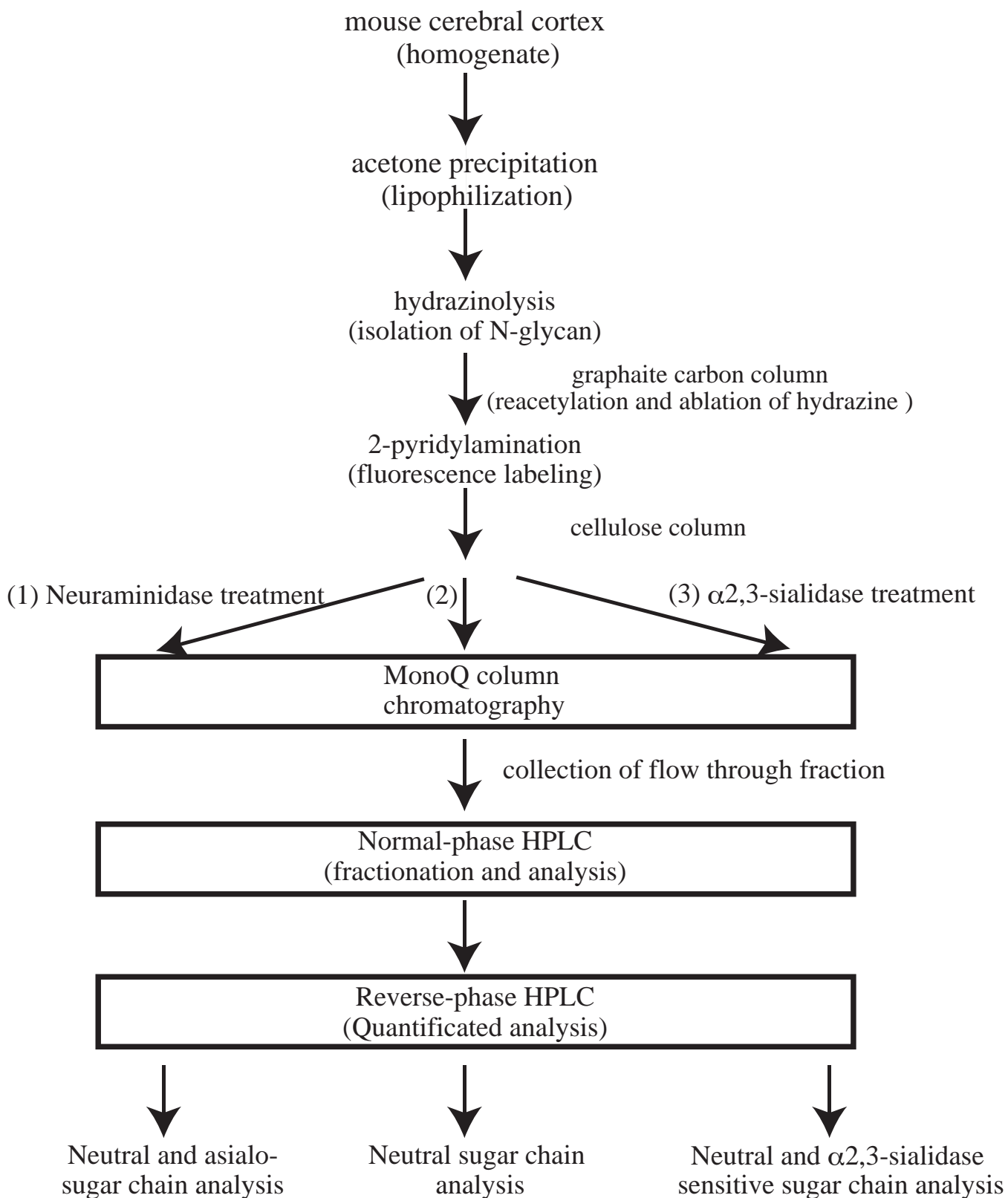


Figure 2

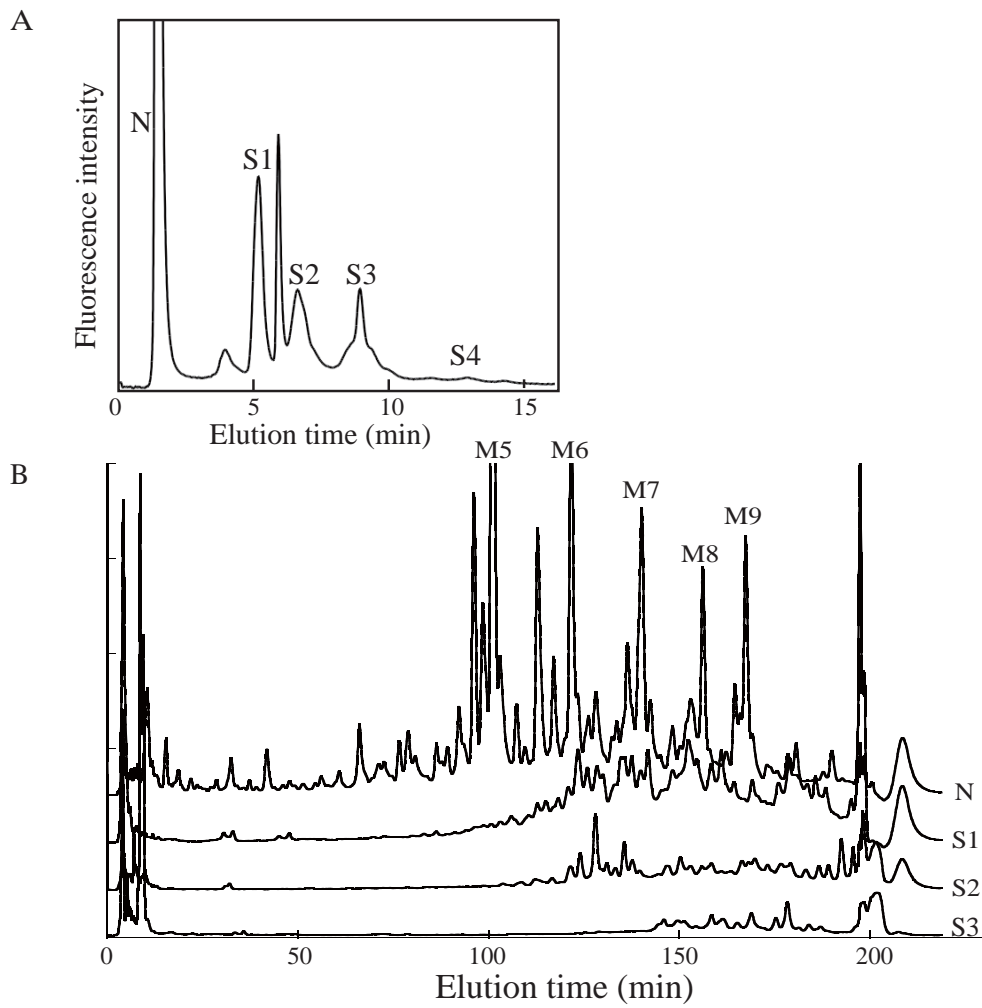
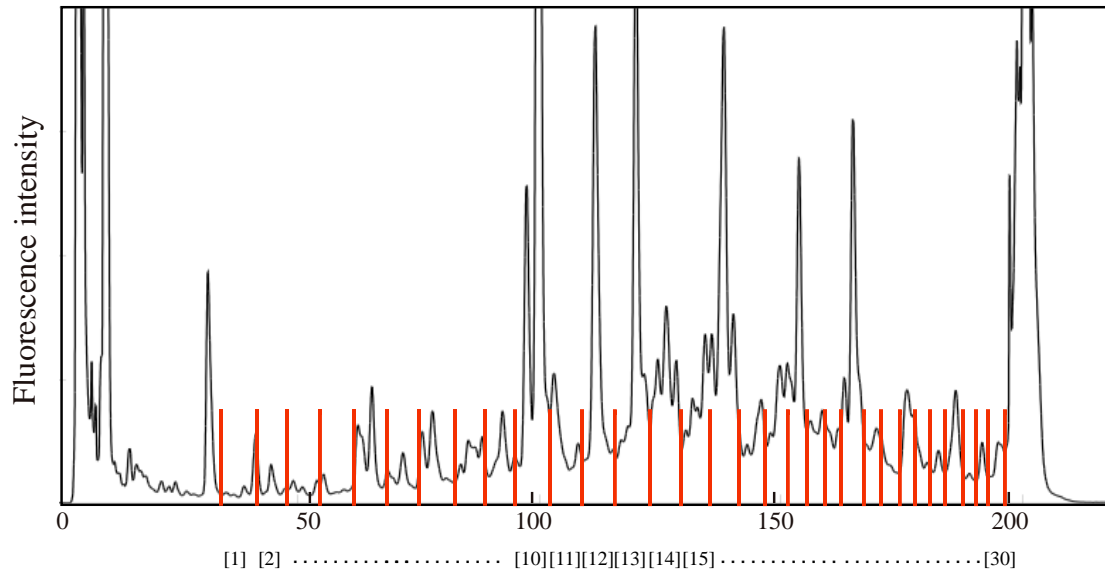


Figure 3

Normal phase HPLC



Reverse phase HPLC analysis

Figure 5

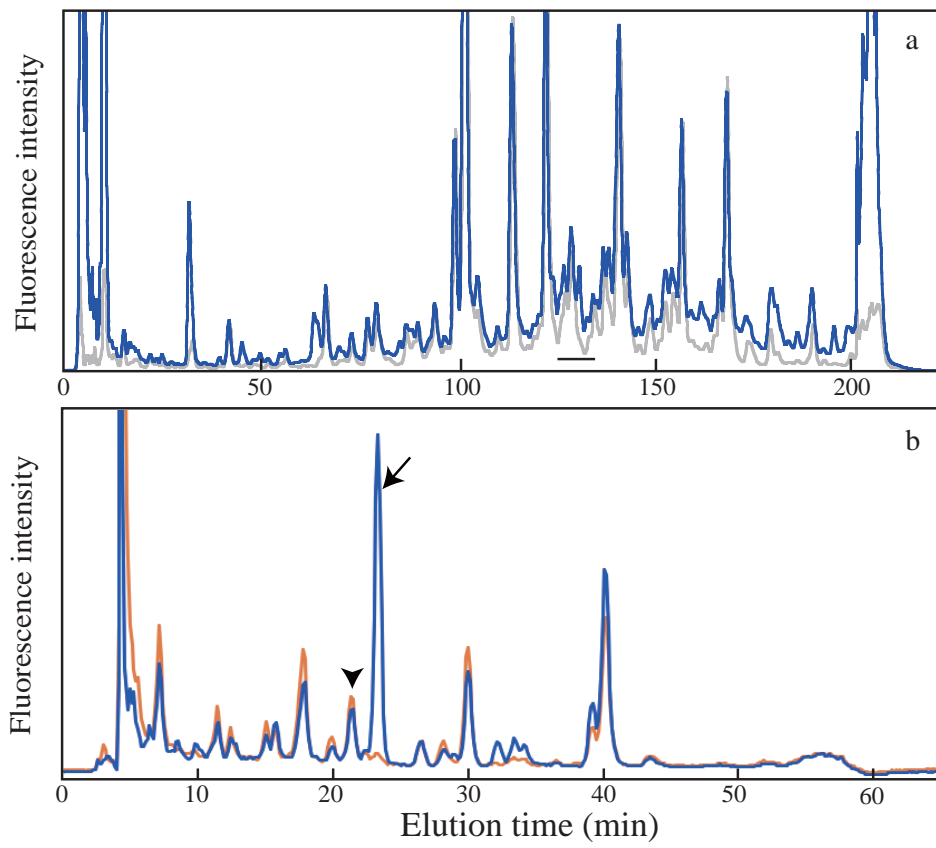


Figure 6

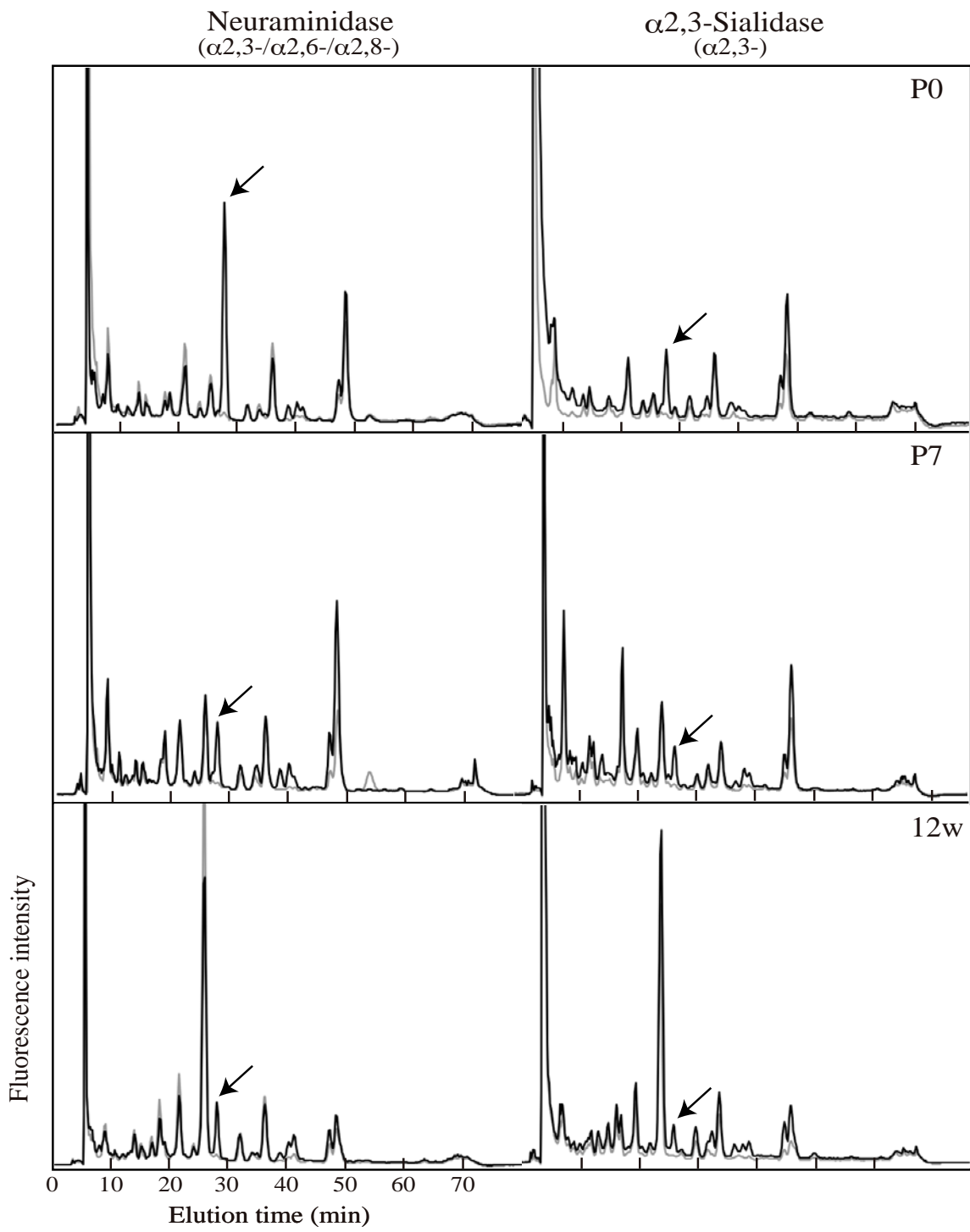


Figure 7

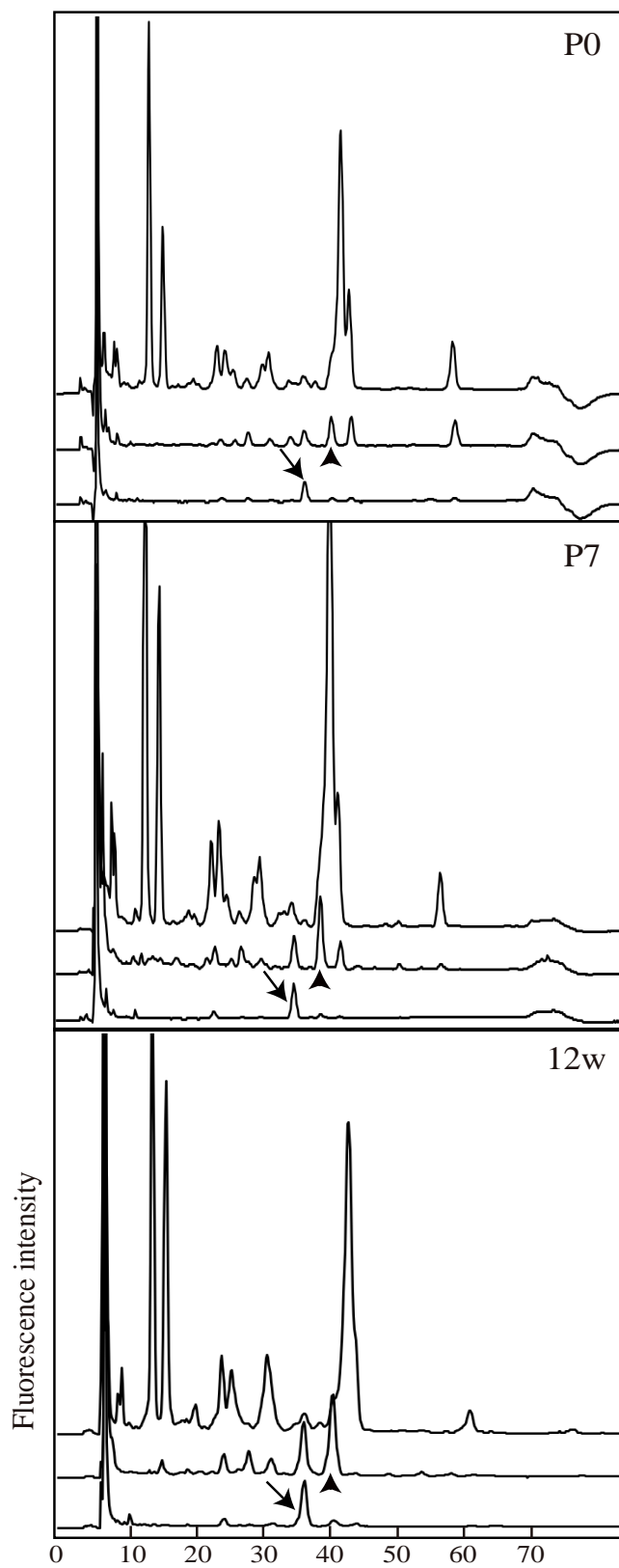
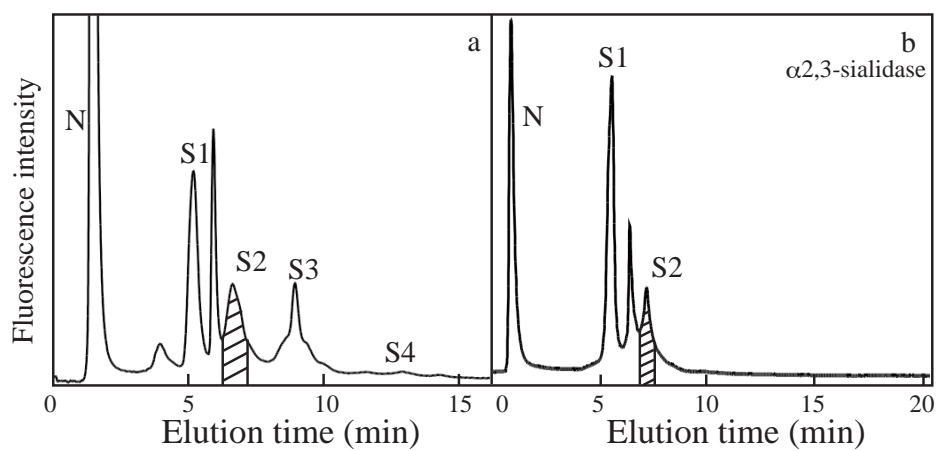
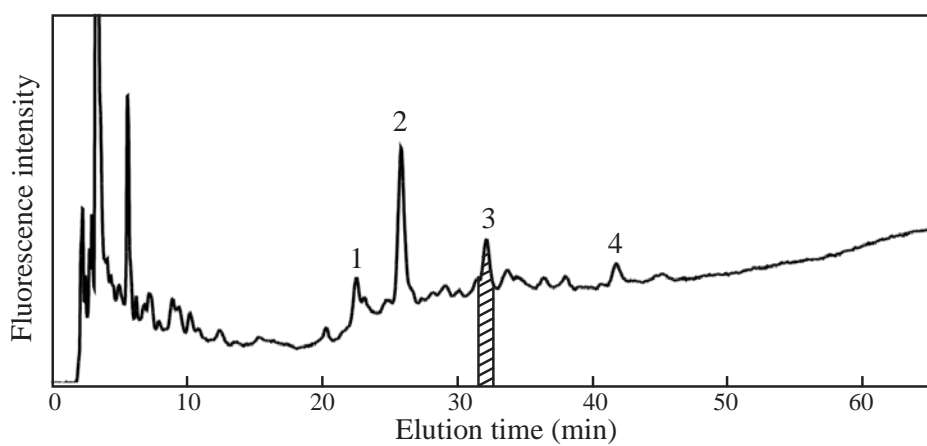


Figure 8

A



B



C

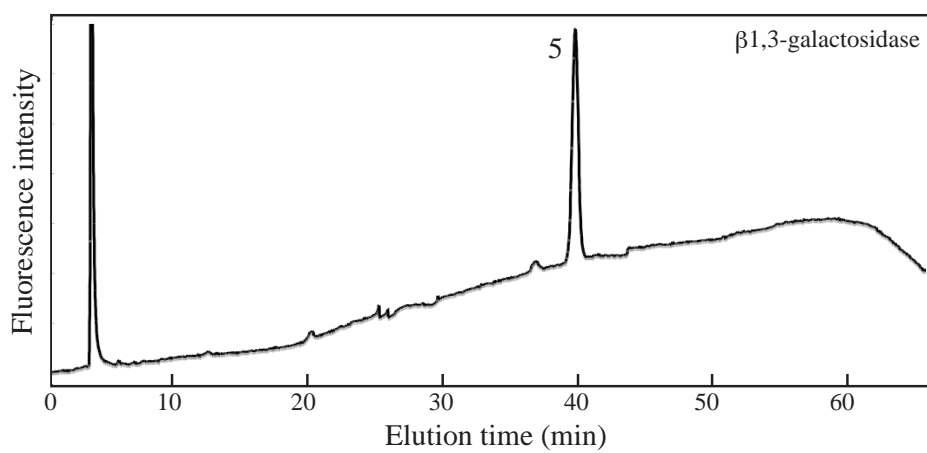
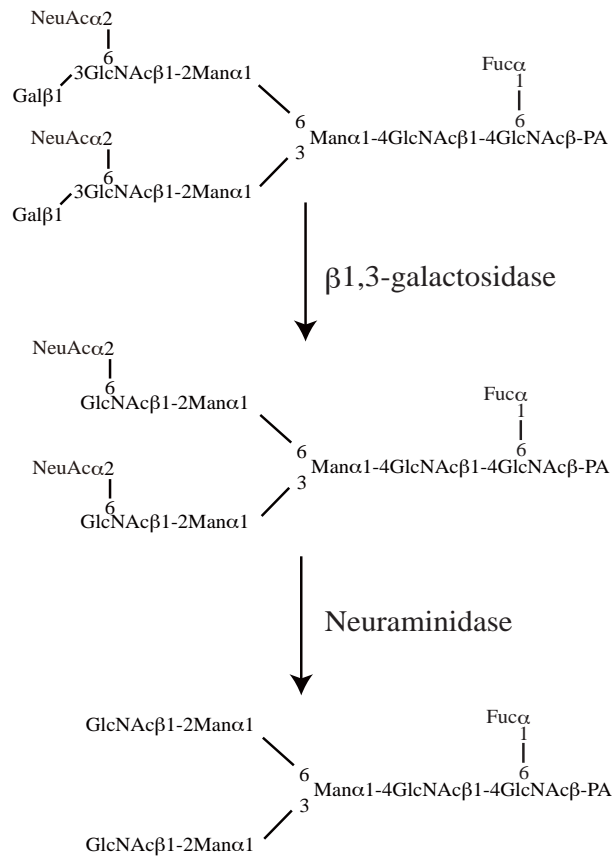


Figure 9



A2G0F

Figure 10

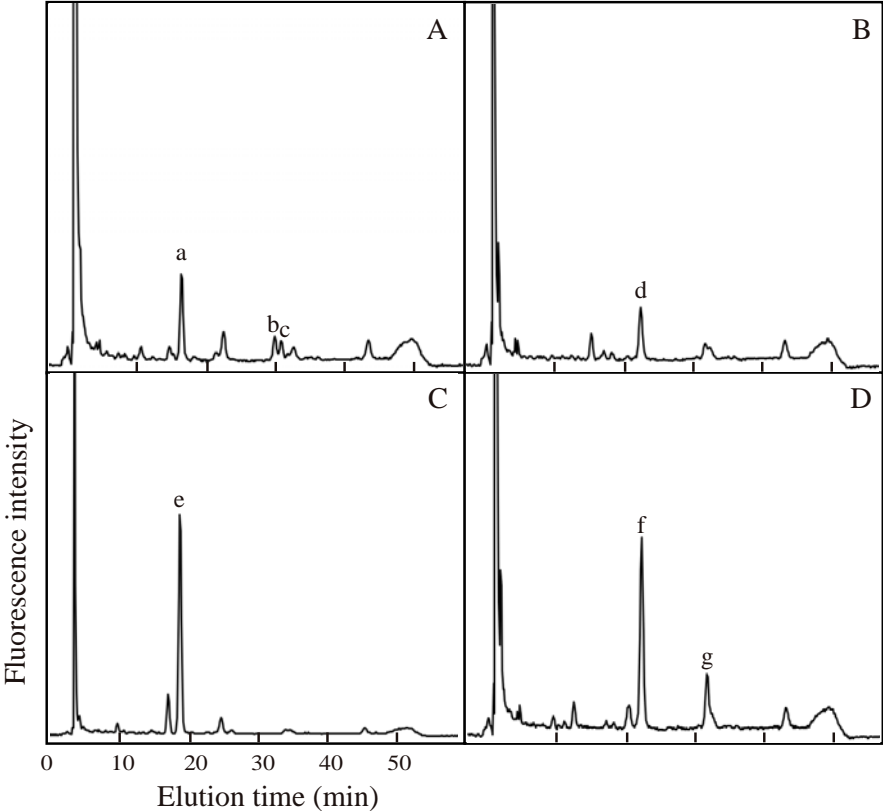


Figure 11

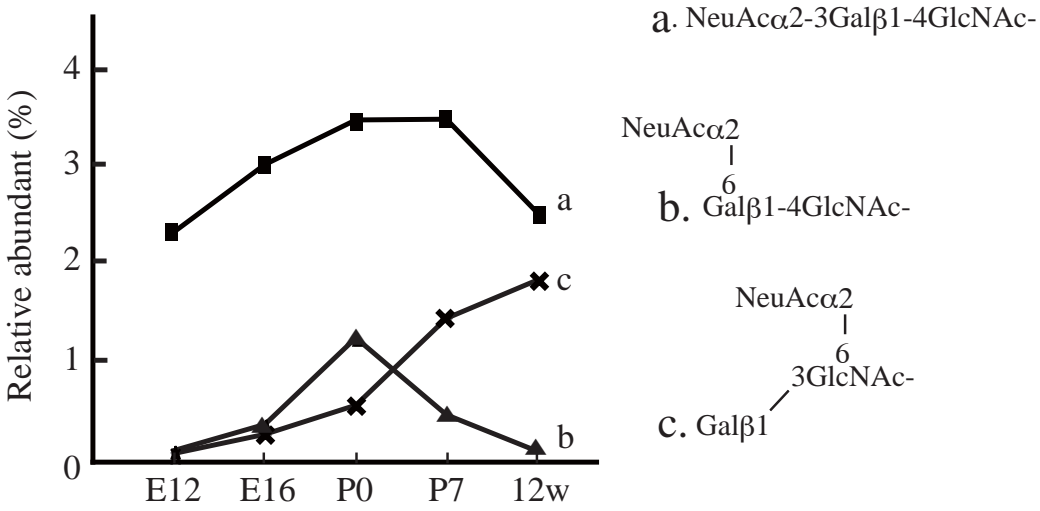


Figure 12

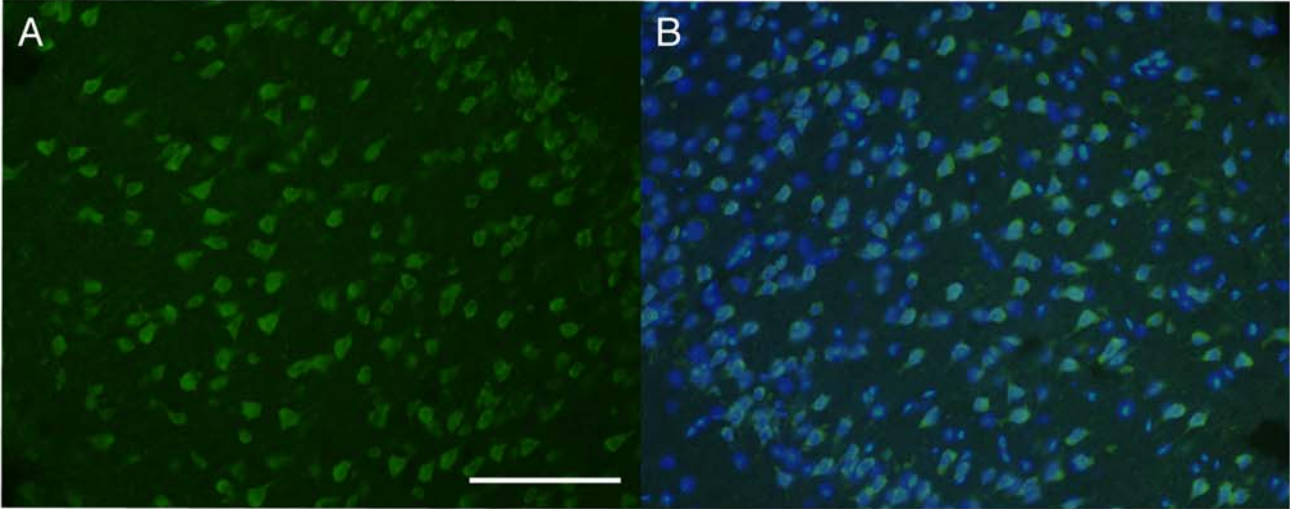


Figure 13-1

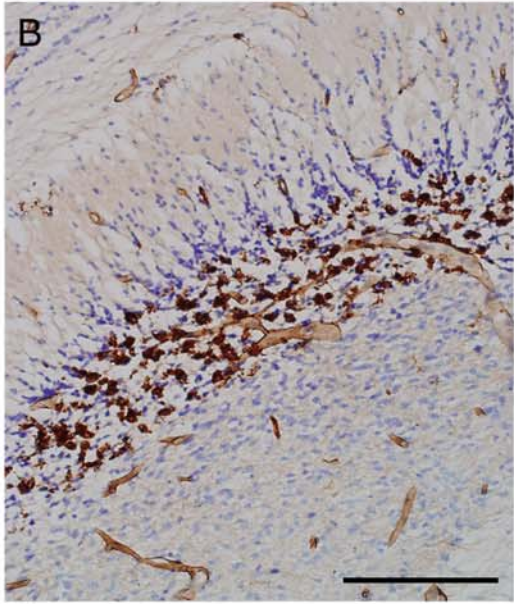
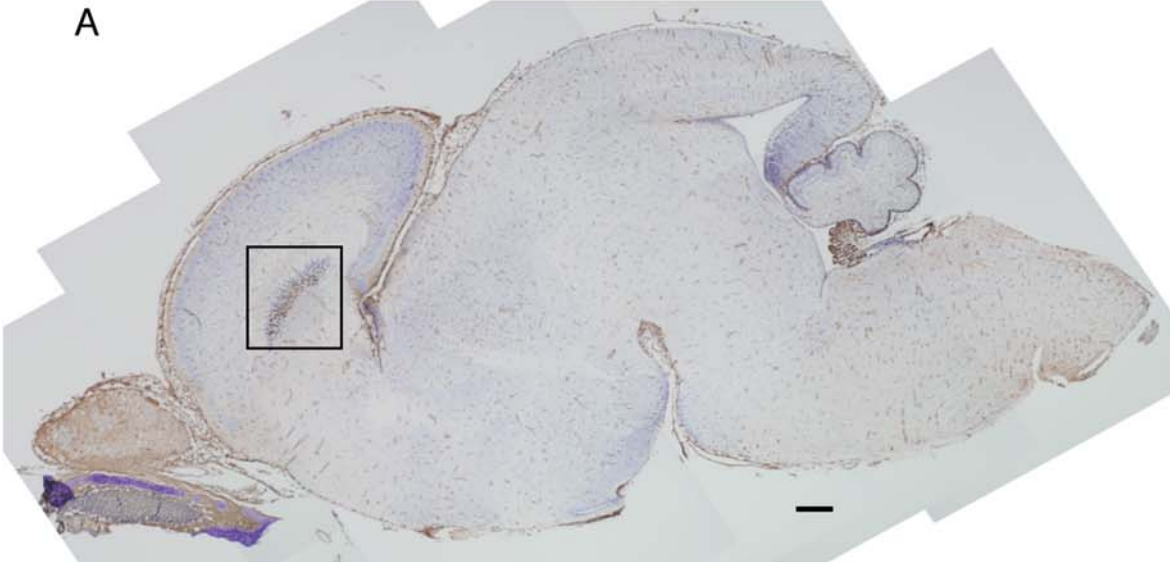


Figure 13-2

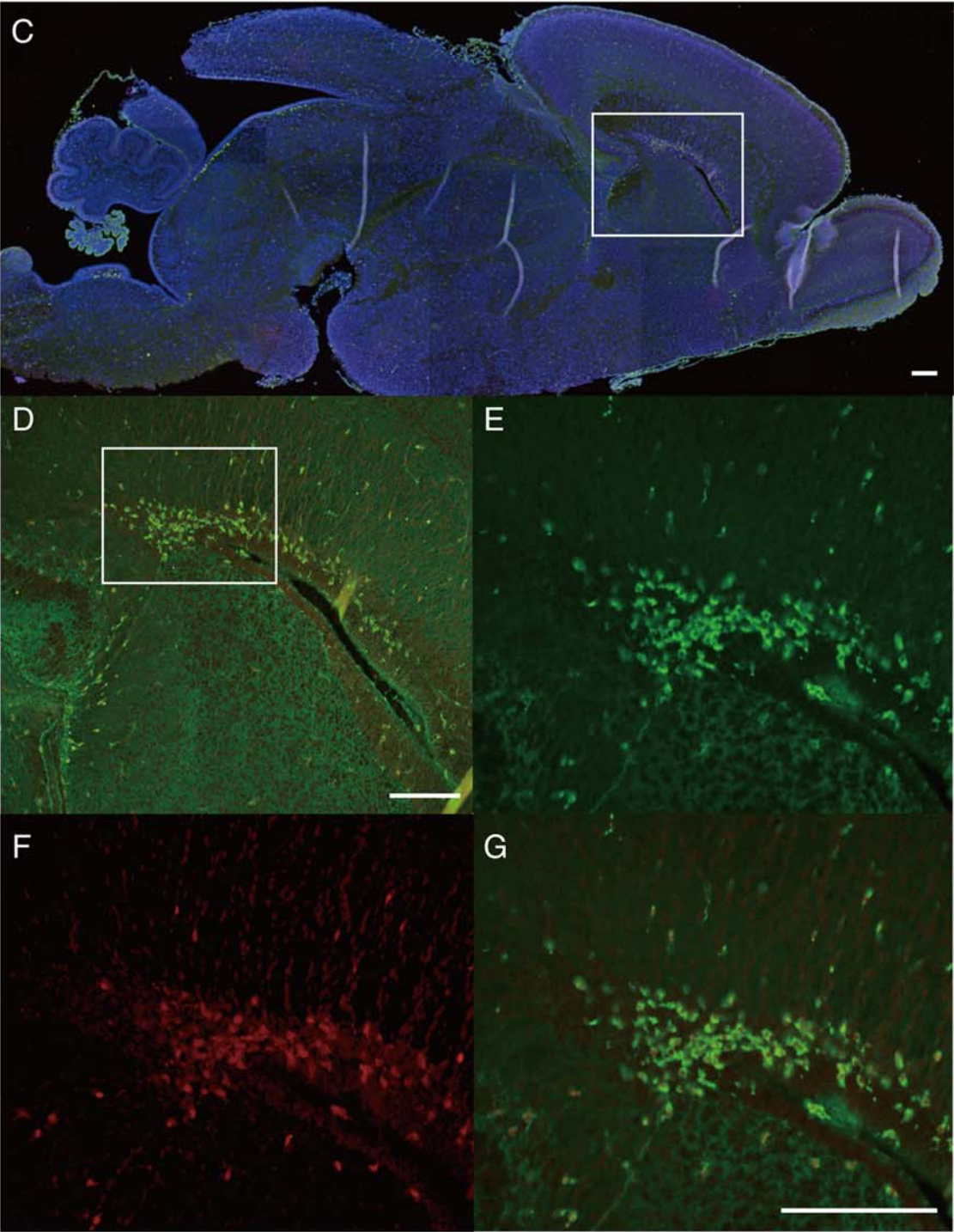


Figure 14

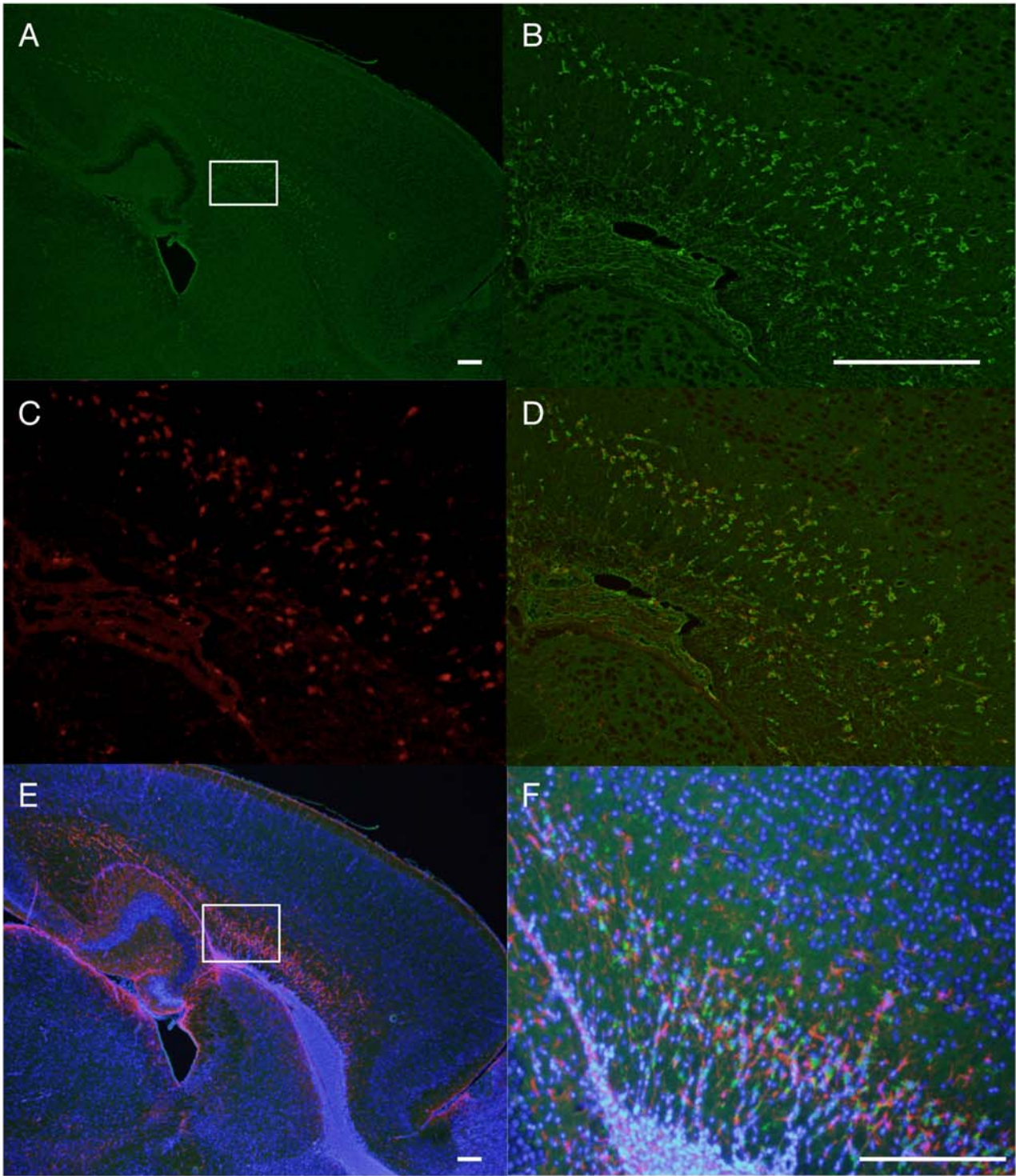


Figure 15

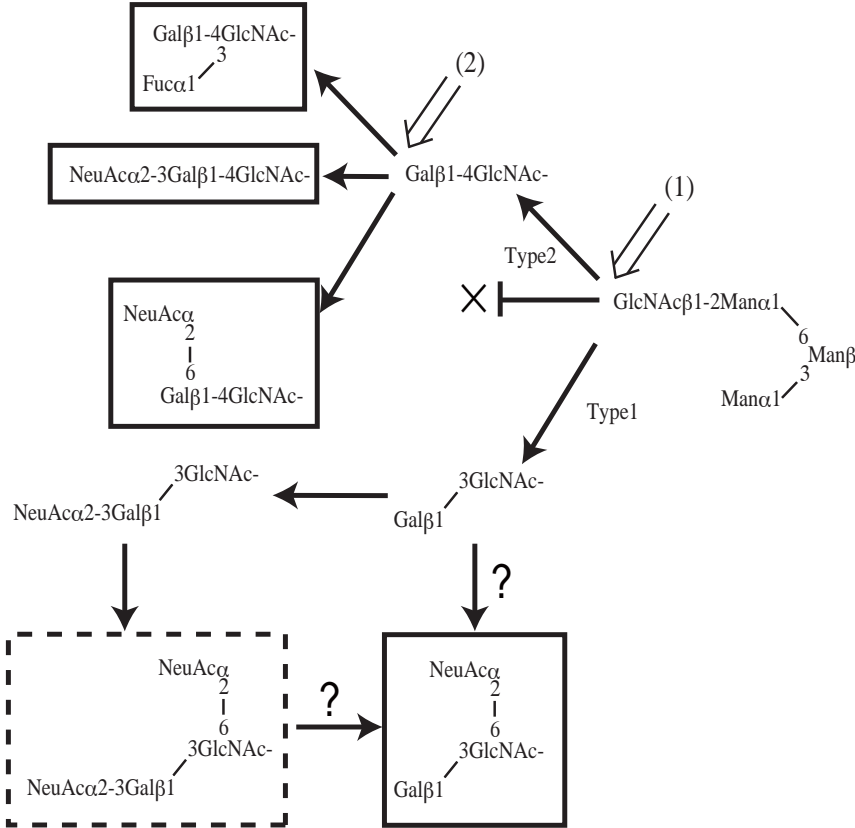


Table 1

The number of sialic acid attached to N-glycans expressed in adult mouse brain

	S1	S2	S3	S4
Structure	G2-BA-2	A2G2		
	Ga+Gb-BA-2	A2G2F		
	A3G3Fo2F	G2-BA2	A4G4F	A4G4F
	X1	A2G1Fo(6)G'1(3)F		
	X2	A2G'2F		
	X3	X3		

S1, S2, S3 and S4 indicate fractions that contain mono-, di-, tri- and tetra-sialyl oligosaccharides, respectively. The Sialylated N-glycans contained in fraction was desialylated and their structure was identified by 2D-HPLC mapping.

Table 2

Proportion of neuraminidase sensitive or sialic acid residue-containing N-glycans in developing and adult cortices

Structure	E12		E16		P0		P7		12w		
	C α 2,3/6/8	C α 2,3									
Gal β 1,4GlcNAc Fuc α 1 (LewisX)	A2G2	100	100	100	100	45.3	100	77.1	100	100	
	A2G2F	100	100	100	88.0	100	76.2	100	79.6	100	92.6
	Ga+Gb-BA-2	61.3	60.5	62.2	61.3	66.2	52.1	87.2	79.5	56.2	55.8
	G2-BA2	52.2	52.2	85.1	65.6	87.9	53.3	87.2	77.4	89.0	86.7
	A4G4F	100	100	100	100	100	100	100	100	100	100
	A2G2Fo(6)F	100	100	100	100	100	100	100	100	100	100
	A2G2Fo(6)FB	88.1	87.9	86.3	86.0	95.4	95.2	94.9	94.7	99.3	98.4
	A3G3Fo2F	N.D	N.D	N.D	N.D	N.D	N.D	N.D	N.D	100	100
	LewisX-H4FB	0	0	0	0	0	0	0	0	0	0
	LewisX-H5F	0	0	0	0	0	0	0	0	0	0
Gal β 1,3GlcNAc (type 1)	LewisX(a+b)-BA-2	0	0	0	0	0	0	0	0	0	
	LewisX2-BA-2	0	0	0	0	0	0	0	0	0	
	A2G1FoF	0	0	0	0	0	0	0	0	0	
	A2G1Fo(6)G'1(3)F	N.D	N.D	N.D	N.D	100	0	100	0	100	0
	A2G'2F	N.D	N.D	N.D	N.D	100	0	100	0	100	0
	A2G1(6)G'1(3)F	N.D	N.D	N.D	N.D	100	0	100	0	100	0

Quantification of neuraminidase or α 2,3-sialidase sensitive component of each sugar chain from cerebral cortices. Each N-glycan pool was divided into three aliquots and each aliquot treated with neuraminidase or α 2,3-sialidase, or untreated, respectively. Each aliquot was then applied to MonoQ HPLC and the flow-through fraction was obtained. N-glycans were separated and quantified using normal phase and reverse phase HPLC. Neuraminidase sensitive component (C α 2,3/6/8) = N-glycan from neuraminidase treated aliquot - that from untreated/N-glycan from neuraminidase treated aliquot $\times 100$ ¹⁾. α 2,3-sialidase sensitive component (C α 2,3) was obtained in a similar manner²⁾. Values present percentage of sialidase sensitive component. The terminal structure of N-glycans is indicated on the extreme left.

$$1) \quad C^{\alpha 2,3/6/8} = \frac{P_D^{\text{Neuraminidase}}}{P_N + P_D} \times 100$$

$$2) \quad C^{\alpha 2,3} = \frac{P_D^{\alpha 2,3\text{-sialidase}}}{P_N + P_D} \times 100$$

Table 3

The number of sialic acid attached to N-glycans after α 2,3-sialidase treatment from developing and adult mouse cortices

	Structure				
	E12	E16	P0	P7	12w
S1	N.D	A2G2F G2-BA-2	A2G2	A2G2	A2G1Fo(6)G'1(3)F A2G1(6)G'1(3)F
			A2G2F	A2G2F	
			Ga+Gb-BA-2	Ga+Gb-BA-2	
			G2-BA-2	G2-BA-2	
			A2G1Fo(6)G'1(3)F	A2G1Fo(6)G'1(3)F	
			A2G'2F	A2G'2F	
A2G1(6)G'1(3)F	A2G1(6)G'1(3)F				
S2	N.D	N.D	A2G2	A2G2	A2G'2F
			A2G2F	A2G2F	
			G2-BA2	G2-BA2	
			A2G'2F	A2G'2F	

S1 and S2 indicate the fractions that usually contain mono- and di-sialyl oligosaccharides, respectively. After α 2,3-sialidase treatment, each anionic fractions were collected and desialylated by neuraminidase. The samples were individually applied to normal-phase and reverse-phase HPLC and identified these structures.